Biointerface Research in Applied Chemistry
Platinum Open Access Journal (ISSN: 2069-5837)

Article
Volume 12, Issue 4, 2022, 5234 - 5265
https://doi.org/10.33263/BRIAC124.52345265

Avoiding the Interaction between S-protein of SARS-CoV-2 and ACE2, to Develop an Adjuvant Antiviral by Molecular Docking

José Luis Vique-Sánchez [1,*]

[1] Mexicali School of Medicine, Autonomous University of Baja California, Mexico
[*] Correspondence: jvique@uabc.edu.mx (J.L.V.-S.);

Scopus Author ID 57195635710

Received: 20.07.2021; Revised: 30.08.2021; Accepted: 5.09.2021; Published: 17.10.2021

Abstract: The COVID-19 pandemic continues today without specific treatment; different treatments have been proposed during this pandemic. This study proposes to develop a new drug by molecular docking, using a library of compounds, almost 500,000 compounds directed to interact in the region between the amino acids (Lys417, Tyr453, Gly496, Gln498, Thr500, Gly502, and Tyr505) in the RBD in S-protein of SARS-CoV-2, to develop a new adjuvant antiviral against COVID-19. It selected ten compounds by molecular docking with a high probability to interact in the specific region in the RBD of SARS-CoV-2 (Lys417, Tyr453, Gly496, Gln498, Thr500, Gly502, and Tyr505), to reduce the interaction with the ACE2. Also, these compounds have a high probability of being safe in humans, validated by web servers of prediction of ADME and toxicity (PreADMET) to develop a new specific adjuvant antiviral against COVID-19.

Keywords: antivirals; RBD; COVID-19; drug by docking; SARS-CoV-2.

1. Introduction

The COVID-19 pandemic continues today without specific treatment; the disease caused by SARS-CoV-2 produces a wide range of signs and symptoms, mainly respiratory, gastrointestinal, and even death [1-4]. Different treatments have been proposed during this pandemic, of the first reports indicating antibiotics and an antiviral (Oseltamivir), but without evidence to effectively fight against COVID-19 [3]. New antivirals with different therapeutic targets have been developed, focusing on RNA-Dependent RNA Polymerase (RdRp), Polyproteins (3CLpro and PLpro) [5-7], Spike Protein (S-protein) [8,9], membrane fusion inhibitors (HR1 and HR2 of S-protein) [10-13] from SARS-CoV-2, or hinder the trimerization of the S-protein of SARS-CoV-2 [14], as well as directed to the ACE2 region that interacts with the RBD [15-19]. Therefore, many works are focusing on developing new drugs against COVID-19, but without results demonstrating an advantage therapeutic yet, which demonstrates the pressing demand for the development of specific drugs against COVID-19.

Due to the SARS-CoV outbreak of 2002, new drugs against therapeutic targets have been developed, where the angiotensin-converting enzyme 2 (ACE2) [20] was identified in the cell membrane, as the interaction region between this type of viruses and human cells; as well as were identified the important amino acids in the region binding domain (RBD) in the S-protein of SARS-CoV for interacting with ACE2. [21].

Recently, another work proposed peptides that could affect the conformation of S-protein and thus hindered the interaction with ACE2 [22]. ACE2 has a role as an important receptor to facilitate this virus to cross the cell membrane and develop its infectious process; even more, today, since it has been reported (December 2020) that there are mutations in RBD that could increase the transmission of this virus and decrease the effect of vaccines [23-25], and the mutation at position 501 (Tyr in instead of Asn) could increase the interaction between S-protein with ACE2. In addition, several works are used as therapeutic targets for the interaction regions between RBD in the S-protein and the ACE2, performing docking for drug repositioning and/or with chemotherapeutic libraries to search drugs or compounds that can inhibit the interaction between RBD with ACE2 [11,22,26,27].

In this study was used the crystallographic structure of the interaction between SARS-CoV-2 (RBD) and ACE2 [28,29] which is demonstrating that the amino acids Lys417, Gly446, Tyr449, Tyr453, Asn487, Gly496, Thr500, Gly502, and Tyr505 in the RBD are very important to interact with ACE2. The crystallographic structure of RBD was used (PDB:6LZG), performing molecular docking directed to the amino acids mentioned, using the EXPRESS-pick Collection of ChembBridge Corp. with almost 500,000 compounds, to determine the compounds that could reduce the interaction between SARS-CoV-2 and ACE2; with these results compounds will be proposed to develop a new drug against COVID-19.

2. Materials and Methods

2.1. Preparation of receptor protein and definition of the binding site.

Atomic coordinates of the Region Binding Domain (RBD) were obtained from the Protein Data Bank (PDB:6LZG). The structure was used as protein targets for docking procedures. The protonation and energy minimization of the PDB file was performed using Molecular Operating Environment (MOE) software with the default parameters and the CHARMM27 force field [30,31]. The region interacts in RBD in amino acids: Lys417, Tyr453, Gly496, Gln498, Thr500, Gly502, and Tyr505 [28].

2.2. Compound library.

The EXPRESS-pick Collection Stock of the small molecule screening library from Chembridge Corp. was used for docking [32]. This collection of small molecule screening compounds contains over 500,000 chemical compounds that fulfill the druggable properties of Lipinski's rules [33,34] and cover a broad area of chemical space.

2.3. Molecular docking.

For molecular docking, following the reported methodology [35,36]. High-throughput virtual molecular docking was carried out [32,37] by the software AutoDock and MOE, using default parameters (Placement: Triangle Matcher, Rescoring 1: London ΔG, Refinement: Forcefield, Rescoring 2: London ΔG, for each ligand up to 100 conformations were generated and saved).

2.4. Calculation of the free binding energy ($\Delta G_{binding}$).

The binding affinity of each complex (Ligand-protein) was estimated by the ratio of General Born *vs.* Volume Integral (GB/VI), using parameters in MOE [38,39]. General Born

or non-bonded interaction energies comprise Van der Waals, Coulomb electrostatic interactions, and implied solvent interaction energies [39].

2.5 Selection of the best ten compounds.

Each compound was simulated with up to 100 conformations, to select the best 10 compounds, the average of the $\Delta G_{binding}$ interaction value of up to 30 conformers of each compound was calculated with Excel (Microsoft-365) following the reported methodology [35,36], the description of chemical properties by PhysChem - ACD/Labs [40], the theoretical toxicity, carcinogenicity, and mutagenicity were considered [41]. The calculated interactions between RBD and the compounds were visualized with Ligand-interaction interactions implemented in MOE.

3. Results and Discussion

3.1. Selection of compounds by docking.

From docking's results, by the interaction of almost 500,000 compounds in the RBD of SARS-CoV-2 (amino acids: Lys417, Tyr453, Gly496, Gln498, Thr500, Gly502, and Tyr505, Figure 1), the selection criteria of the best compounds were based on the calculation of the average of the $\Delta G_{binding}$ of each compound, using the values of conformers (23 to 30 conformers), determining an average range from -5.81 to -6.21 kcal/mol^{-1} for the best compounds (Table 1, and details on the supplementary material Table S1). We selected 10 compounds depicted here as R1 to R10 from the Express-pick Collection Stock of the small molecule screening of Chembridge library (ChemBridge Corp.), and the analysis of the interaction of each compound with RBD was carried out with the interaction report (Table 2 and details in Table S2 – S11). Afterward, the theoretical toxicity was evaluated with two websites (Prediction of Toxicity and PreADMET web server, prediction of carcinogenicity and mutagenicity).

The description of the theoretical toxicity (Table S12), ADME characteristics (Table S13), and chemical properties of each compound (R1– R10, Table S14), are presented in the supplemental material.

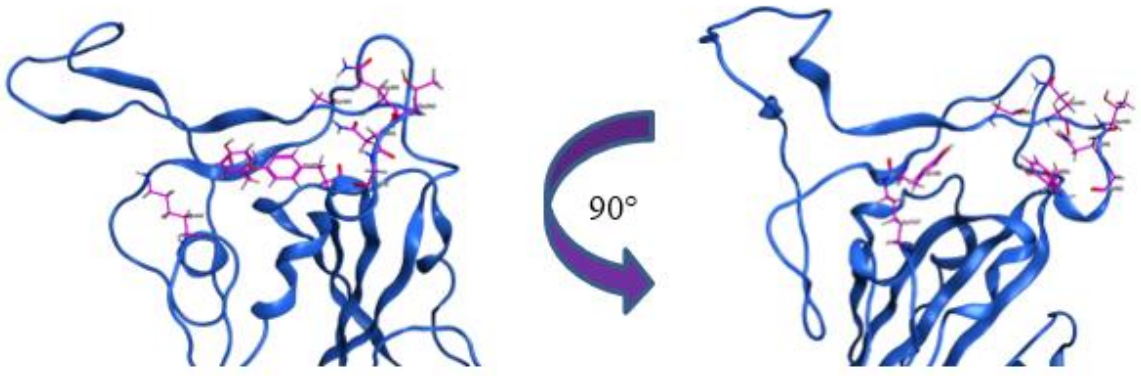

Figure 1. RBD (Blue) shows amino acids Lys417, Tyr453, Gly496, Gln498, Thr500, Gly502, and Tyr505 (Pink), as regions chosen for docking.

Table 1. ID ChemBridge Corp., chemical name and structure of 10 best compounds, R1 to R10.

R1.- 7782385, N,N'-9H-Fluorene-2,7-diylbis[2-(3,4-dimethoxyphenyl)acetamide] 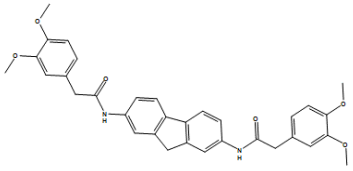	**R2.-** 5543060**,** N,N'-bis{4-methyl-2-[(4-methylphenyl)diazenyl]phenyl}isophthalamide 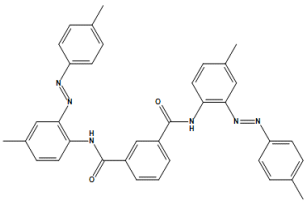
R3.- 6532012**,** 3,5-Bis{[(2-methoxyphenoxy)acetyl]amino}-N-(2-methyl-2-propanyl)benzamide 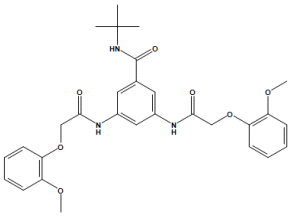	**R4**.- 6363182, N,N'-4,4'-Biphenyldiylbis[2-(4-methylphenoxy)acetamide] 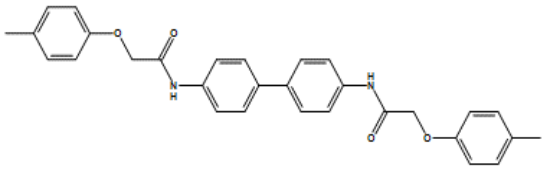
R5.- 699027, (2E)-N-(4-{4-Methyl-5-[(1-naphthylmethyl)sulfanyl]-4H-1,2,4-triazol-3-yl}phenyl)-3-phenylacrylamide 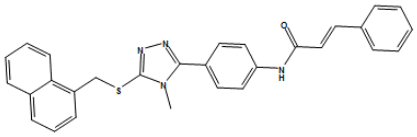	**R6.-** 7845819 N-Benzyl-2-{[({5-[(4-methoxyphenoxy)methyl]-4-methyl-4H-1,2,4-triazol-3-yl}sulfanyl)acetyl]amino}-4,5,6,7-tetrahydro-1-benzothiophene-3-carboxamide 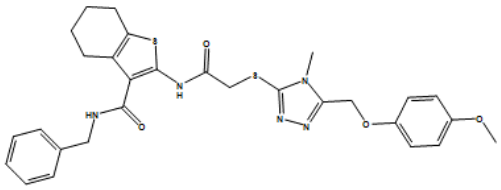
R7.- 5837947, 4-{[4-({4-[(E)-(3-Allyl-4-oxo-2-thioxo-1,3-thiazolidin-5-ylidene)methyl]-2-methoxyphenoxy}methyl)benzyl]oxy}-3-methoxybenzaldehyde 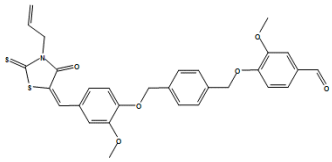	**R8.-** 5471668 N,N'-[(2-Phenyl-4,6-pyrimidinediyl)di-4,1-phenylene]bis[2-(2-thienyl)acetamide] 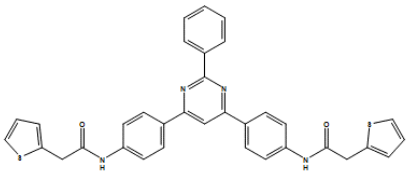
R9.- 7779797, N,N'-[Methylenebis(2-hydroxy-4,1-phenylene)]bis[2-(2-methoxyphenoxy)acetamide] 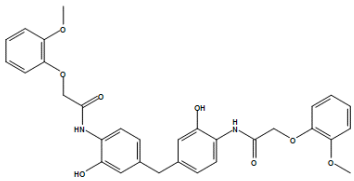	**R10**.- 5730468, (2Z,5Z)-3-Benzyl-2-(benzylimino)-5-{3-methoxy-4-[(4-nitrobenzyl)oxy]benzylidene}-1,3-thiazolidin-4-one 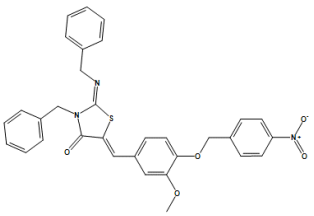

Table 2. ID compound, Smile, Interaction with residues in RBD, Number of conformers used, $\Delta G_{binding}$ average (kcal/mol-1) with standard deviation (SD), Ames test and strain used (positive or negative) [43].

Compound ID Chembridge Corp.	**Smile**	**Interaction with residues in ACE2 (Table S1 – S20)**	**Number of conformers**	**Average of $\Delta G_{binding}$ and SD**	**PreADMET Ames test -TA100_10RL -TA100_NA -TA1535_10R -TA1535_NA**
R1.- 7782385	COc1ccc(cc1OC)CC(=O)Nc2ccc-3c(c2)Cc4c3ccc(c4)NC(=O)Cc5ccc(c(c5)OC)OC	Arg403, Glu406, Gly416, Lys417, Tyr449, Gly496, Gln498, Tyr505	25	-6.21 ± 0.62	Mutagen y -Negative -Negative -Negative -Negative
Compound ID Chembridge Corp.	**Smile**	**Interaction with residues in ACE2 (Table S1 – S20)**	**Number of conformers**	**Average of $\Delta G_{binding}$ and SD**	**PreADMET Ames test -TA100_10RL -TA100_NA -TA1535_10R -TA1535_NA**
R2.- 5543060	Cc1ccc(cc1)N=Nc2cc(ccc2NC(=O)c3cccc(c3)C(=O)Nc4ccc(cc4N=Nc5ccc(cc5)C)C)C	Lys417, Tyr449, Tyr453, Leu455, Phe456, Gln493, Tyr495, Gly496, Gln498, Thr500, Gly502, Tyr505	28	-5.91 ± 0.46	Mutagen -Positive -Negative -Negative -Negative
R3.- 6532012	CC(C)(C)NC(=O)c1cc(cc(c1)NC(=O)COc2ccccc2OC)NC(=O)COc3ccccc3OC	Arg403, Arg408, Gly416, Lys417, Gln493, Tyr495, Gly496, Gln498, Gly502	23	-5.88 ± 0.57	Non mutagen -Negative -Negative -Negative -Negative
R4.- 6363182	Cc1ccc(cc1)OCC(=O)Nc2ccc(cc2)c3ccc(cc3)NC(=O)COc4ccc(cc4)C	Arg403, Glu406, Thr415, Lys417, Gly446, Tyr449, Tyr453, Gly496, Gly502	23	-5.84 ± 0.44	Non mutagen -Negative -Negative -Negative -Negative
R5.- 699027	Cn1c(nnc1SCc2cccc3c2cccc3)c4ccc(cc4)NC(=O)/C=C/c5ccccc5	Arg403, Glu406, Gly416, Lys417, Gly446, Tyr449, Gly496, Gln498	27	-5.83 ± 0.52	Mutagen -Negative -Negative -Negative -Negative
R6.- 7845819	Cn1c(nnc1SCC(=O)Nc2c(c3c(s2)CCCC3)C(=O)NCc4ccccc4)COc5ccc(cc5)OC	Arg403, Arg408, Gly416, Lys417, Tyr449, Tyr453, Asn460, Gln493, Ser494, Tyr505	28	-5.83 ± 0.43	Non mutagen -Negative -Negative -Negative -Negative
R7.- 5837947	COc1cc(ccc1OCc2ccc(cc2)COc3ccc(cc3OC)C=O)/C=C/4\C(=O)N(C(=S)S4)CC=C	Arg403, Glu406, Arg408, Gly416, Lys417, Gly446, Tyr449, Tyr453, Gly496, Gln498, Thr500, Gly502, Tyr505	26	-5.83 ± 0.49	Mutagen -Negative -Negative -Negative -Negative
R8.- 5471668	c1ccc(cc1)c2nc(cc(n2)c3ccc(cc3)NC(=O)Cc4cccs4)c5ccc(cc5)NC(=O)Cc6cccs6	Arg403, Glu406, Gln409, Thr415, Lys417, Asp420, Tyr449, Tyr453, Gly496, Gln498, Thr500, Gly502, Glu504, Tyr505	25	-5.82 ± 0.41	Mutagen -Negative -Negative -Negative -Negative
R9.- 7779797	COc1ccccc1OCC(=O)Nc2ccc(cc2O)Cc3ccc(c(c3)O)NC(=O)COc4ccccc4OC	Arg403, Lys417, Gly446, Tyr449, Tyr453, Ala475, Ser494, Tyr495, Gly496, Gln498, Thr500, Gly502, Tyr505	30	-5.82 ± 0.56	Non mutagen -Negative -Negative -Negative -Negative
R10.- 5730468	COc1cc(ccc1OCc2ccc(cc2)[N+](=O)[O-])/C=C\3/C(=O)N(/C(=N/Cc4ccccc4)/S3)Cc5ccccc5	Arg403, Arg408, Gln409, Gly416, Lys417, Tyr449, Tyr453, Gly496, Gly502, Tyr505	26	-5.81 ± 0.47	Mutagen -Positive -Negative -Negative -Negative

3.2. Interaction of compounds R1 – R10 with RBD.

To describe the probable interaction sites between each compound (R1 – R10) with RBD, we analyzed up to 30 conformers of each compound with the better $\Delta G_{binding}$ average values of interaction in amino acids Lys417, Tyr453, Gly496, Gln498, Thr500, Gly502, and Tyr505 (Figure 1). From the docking result (Table S2 – S11), we determined the main amino acids in RBD to interact with the ten compounds. These are Arg403, Glu406, Arg408, Gln409, Thr415, Lys417, Asp420, Gly446, Tyr449, Tyr453, Leu455, Asn460, Ala475, Gln493, Ser494, Tyr495, Gly496, Gln498, Thr500, Gly502, Glu504, and Tyr505 (Table 2). The interaction of each compound and its conformers with RBD are shown in the supplementary material (Figure S2 – S16).

3.3. Discussion.

Research continues to create a specific drug against SARS-CoV-2, proposing a different way to attack COVID-19 to combat the pandemic that continues to develop today. Despite the large number of works reported on new antivirals and compounds targeting SARS-CoV-2, there is still no 100% effective treatment. The development of an effective treatment against COVID-19 is still under development in the world [11-13,17-19] synthetic peptides that induced conformational changes in the structure at S-protein of SARS-CoV-2 [22], characterizing and proposing potential targets for the interaction between SARS-CoV-2 and ACE2 [17,44] as well as directed to the ACE2 region that interacts with the RBD [15,16].

In this study, it was carried out a molecular docking aimed at the reported amino acids in the RBD of SARS-CoV-2 (Lys417, Tyr453, Gly496, Gln498, Thr500, Gly502, and Tyr505), that is important to interact with ACE2 [28,45], it was determined that residues Arg403, Glu406, Arg408, Gln409, Thr415, Lys417, Asp420, Gly446, Tyr449, Tyr453, Leu455, Asn460, Ala475, Gln493, Ser494, Tyr495, Gly496, Gln498, Thr500, Gly502, Glu504, and Tyr505 are important for the ten compounds that are proposed to interact with the RBD (Table 2), in addition, it has been reported that these amino acids are very important for the interaction between SARS-CoV-2 with ACE2 [20,21,28,45].

The docking results determined several interactions with hydrogen bridges of each compound proposed in the region where is the amino acid Asn501 (Table S2). It is important to emphasize that the interaction of this area with ACE2 could be prevented since that currently identified mutations in RBD that could increase the infectious process and decrease the effect of vaccines [23,24,25]. The mutation in position 501 in the S-protein (Tyr instead of Asn) is proposed as a factor that could increase the interaction of RBD with ACE2. Therefore, this site of interaction in ACE2 today retakes greater importance as a therapeutic target to inhibit the interaction between ACE2 and RBD (Figure 2).

The methodology followed for molecular docking has good results, previously demonstrated to the development of new drugs [35,46-48] even with patents granted of compounds against *T. vaginalis* [49]. For the selection of the best compounds, up to 30 conformers of each compound were analyzed, this gives us a greater probability of choosing the compounds that could interact in the amino acids Lys417, Tyr453, Gly496, Gln498, Thr500, Gly502, and Tyr505 in RBD (Figure 1), in addition, the compounds chosen are validated through two toxicity prediction web servers (Table 2 and Table S12). Thus, this could reduce the time that must be waited for to be used in humans. Therefore, we propose

compounds (R1 – R10) with a high probability to be safe in humans, which could be tested at *in vitro* tests interaction of S-protein SARS-CoV-2 with ACE2.

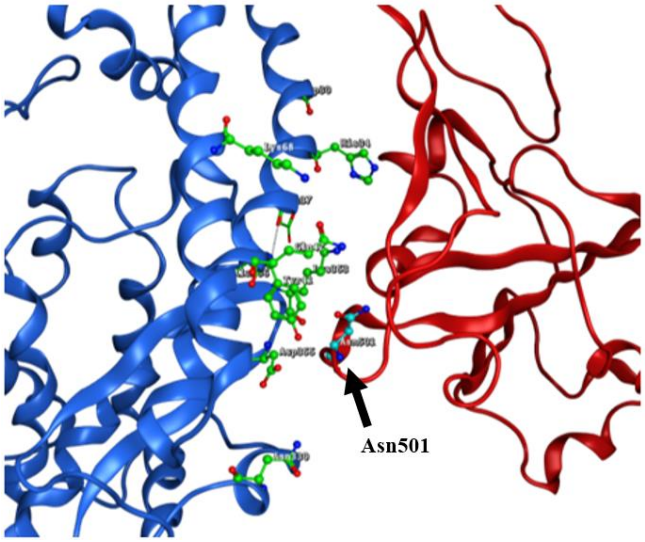

Figure 2. ACE2 (Blue) shows residues Gln24, Asp30, His34, Tyr41, Gln42, Met82, Asp330, Lys353, and Asp355 (Green). RBD of SARS-CoV-2 (Red) and Asn501 (Cyan) interacting with ACE2.

On the other hand, the new treatments could be by compounds that are directed towards the interaction regions between RBD and ACE2. This could increase the inhibitory effect and decrease the infectious process of SARS-CoV-2. Using these ten compounds in combination with some of the compounds that are already proposed against ACE2 [15,16] could stop the virus interaction with the cell receptor and thus block the formation of the RBD-ACE2 complex (Figure 3).

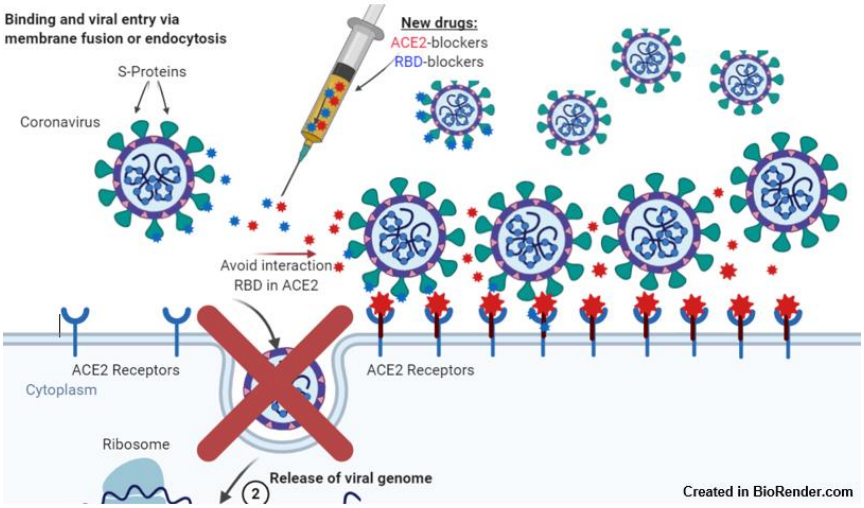

Figure 3. Combination of specific compounds that interact with the RBD of SARS-CoV-2 and ACE2 inhibits the interaction between SARS-CoV-2 and ACE2.

The proposed compounds do not have a specific use against COVID-19, nor a scientific article or registered patent. All the compounds are available to acquire them, perform *in vitro* assays, and determine the effect on the interaction in the RBD of SARS-CoV-2 with ACE2.

4. Conclusions

This study proposes ten highly probability compounds to interact in the specific region in the RBD of SARS-CoV-2 (Lys417, Tyr453, Gly496, Gln498, Thr500, Gly502, and Tyr505),

in order to reduce the interaction with the ACE2. These ten compounds are highly likely to be safe in humans since they were validated by the PreADMET server (ADME and Toxicity Predictor). These ten compounds are available at many pharmaceutical compounds synthesis companies worldwide. To continue development at *in vitro* assays, determine the effect of these compounds on the RBD of SARS-CoV-2 and develop a new specific adjuvant antiviral against COVID-19 that helps combat this pandemic providing the opportunity to give a new direction to global health.

Funding

This research received no external funding.

Acknowledgments

The author is very grateful for the financial support from PTC 880-PRODEP-SEP, SNI-CONACyT, FMM-UABC, CISALUD-UABC, and Dr. José Manuel Avendaño Reyes.

Conflicts of Interest

The author declares no conflict of interest.

References

1. Zhao, J.; Li, X.; Gao, Y.; Huang, W. Risk factors for the exacerbation of patients with 2019 Novel Coronavirus: A meta-analysis. *Int. J. Med. Sci.* **2020**, *17*, 1744–1750, http://doi.org/10.7150/ijms.47052.
2. De Wit, E.; van Doremalen, N.; Falzarano, D.; Munster, V.J. SARS and MERS: recent insights into emerging coronaviruses. *Nat. Rev. Microbiol.* **2016**, *14*, 523–34, http://doi.org/10.1038/nrmicro.2016.81.
3. Guan, W.-J.; Ni, Z.-y.; Hu, Y.; Liang, W.; Ou, C.-Q.; He, J.-x.; Liu, L.; Shan, H.; Lei, C.-l.; Hui, D.; Du, B.; Li, L-J., Zeng, G., Yuen, K-Y., Chen, R.; Tang, C.; Wang, T.; Chen, P.; Xiang, J.; Li, S.; Wang, J.; Liang, Z.; Peng, Y.; Wei, L.; Liu, Y.; Hu, Y.; Peng, P.; Wang, J-M.; Liu, J.; Chen, Z.; Li, G.; Zheng, Z-J.; Qiu, S.; Luo, J.; Ye, C-J.; Zhu, S-Y.; Zhong, N-S. Clinical Characteristics of Coronavirus Disease 2019 in China. *New England Journal of Medicine* **2020**, *382*, http://doi.org/10.1056/NEJMoa2002032.
4. Hu, Y.; Sun, J.; Dai, Z.; Deng, H.; Li, X.; Huang, Q.; Wu, Y.; Sun, L.; Xu, Y. Prevalence and severity of corona virus disease 2019 (COVID-19): A systematic review and meta-analysis. *J. Clin. Virol.* **2020**, *127*, 104371, http://doi.org/10.1016/j.jcv.2020.104371.
5. Wang, M.; Cao, R.; Zhang, L.; Yang, X.; Liu, J.; Xu, M.; Shi, Z.; Hu, Z.; Zhong, W.; Xiao, G. Remdesivir and chloroquine effectively inhibit the recently emerged novel coronavirus (2019-nCoV) in vitro. *Cell Res.* **2020**, *30*, 269–271, http://doi.org/10.1038/s41422-020-0282-0.
6. Sheahan, T.P.; Sims, A.C.; Leist, S.R.; Schäfer, A.; Won, J.; Brown, A.J.; Montgomery, S.A.; Hogg, A.; Babusis, D.; Clarke, M.O.; Spahn, J.E.; Bauer, L.; Sellers, S.; Porter, D.; Feng, J.Y.; Cihlar, T.; Jordan, R.; Denison, M.R.; Baric, R.S. Comparative therapeutic efficacy of remdesivir and combination lopinavir, ritonavir, and interferon beta against MERS-CoV. *Nat. Commun.* **2020**, *11*, 222, http://doi.org/10.1038/s41467-019-13940-6.
7. Li, G.; De Clercq, E. Therapeutic options for the 2019 novel coronavirus (2019-nCoV). *Nat. Rev. Drug Discov.* **2020**, *19*, 149–150, http://doi.org/10.1038/d41573-020-00016-0.
8. Calligari, P.; Bobone, S.; Ricci, G.; Bocedi, A. Molecular Investigation of SARS–CoV-2 Proteins and Their Interactions with Antiviral Drugs. *Viruses* **2020**, *12*, 445, http://doi.org/10.3390/v12040445.
9. Huang, J.; Song, W.; Huang, H.; Sun, Q. Pharmacological Therapeutics Targeting RNA-Dependent RNA Polymerase, Proteinase and Spike Protein: From Mechanistic Studies to Clinical Trials for COVID-19. *J. Clin. Med.* **2020**, *9*, 1131, http://doi.org/10.3390/jcm9041131.
10. Iftikhar, H.; Ali, H.N.; Farooq, S.; Naveed, H.; Shahzad-ul-Hussan, S. Identification of potential inhibitors of three key enzymes of SARS-CoV2 using computational approach. *Comput. Biol. Med.* **2020**, *122*, 103848, http://doi.org/10.1016/j.compbiomed.2020.103848.

11. Wu, C.; Liu, Y.; Yang, Y.; Zhang, P.; Zhong, W.; Wang, Y.; Wang, Q.; Xu, Y.; Li, M.; Li, X.; Zheng, M.; Chen, L.; Li, H. Analysis of therapeutic targets for SARS-CoV-2 and discovery of potential drugs by computational methods. *Acta Pharm. Sin. B* **2020**, *10*, 766–788, http://doi.org/10.1016/j.apsb.2020.02.008.
12. Xia, S.; Yan, L.; Xu, W.; Agrawal, A.S.; Algaissi, A.; Tseng, C.-T.K.; Wang, Q.; Du, L.; Tan, W.; Wilson, I.A.; Jiang, S.; Yang, B.; Lu, L. A pan-coronavirus fusion inhibitor targeting the HR1 domain of human coronavirus spike. *Sci. Adv.* **2019**, *5*, eaav4580, http://doi.org/10.1126/sciadv.aav4580.
13. Xia, S.; Liu, M.; Wang, C.; Xu, W.; Lan, Q.; Feng, S.; Qi, F.; Bao, L.; Du, L.; Liu, S.; Qin, C.; Sun, F.; Shi, Z.; Zhu, Y.; Jiang, S.; Lu, L. Inhibition of SARS-CoV-2 (previously 2019-nCoV) infection by a highly potent pan-coronavirus fusion inhibitor targeting its spike protein that harbors a high capacity to mediate membrane fusion. *Cell Res.* **2020**, *30*, 343–355, http://doi.org/10.1038/s41422-020-0305-x.
14. Vankadari, N. Arbidol: A potential antiviral drug for the treatment of SARS-CoV-2 by blocking trimerization of the spike glycoprotein. *Int. J. Antimicrob. Agents* **2020**, 105998, http://doi.org/10.1016/j.ijantimicag.2020.105998.
15. Benítez-Cardoza, C.G.; Vique-Sánchez, J.L. Potential inhibitors of the interaction between ACE2 and SARS-CoV-2(RBD), to develop a drug. *Life Sci.* **2020**, *256*, 117970, http://doi.org/10.1016/j.lfs.2020.117970.
16. Khelfaoui, H.; Harkati, D.; Saleh, B.A. Molecular docking, molecular dynamics simulations and reactivity, studies on approved drugs library targeting ACE2 and SARS-CoV-2 binding with ACE2. *J. Biomol. Struct. Dyn.* **2020**, 1–17, http://doi.org/10.1080/07391102.2020.1803967.
17. Grifoni, A.; Sidney, J.; Zhang, Y.; Scheuermann, R.H.; Peters, B.; Sette, A. A Sequence Homology and Bioinformatic Approach Can Predict Candidate Targets for Immune Responses to SARS-CoV-2. *Cell Host Microbe* **2020**, http://doi.org/10.1016/j.chom.2020.03.002.
18. Ton, A.-T.; Gentile, F.; Hsing, M.; Ban, F.; Cherkasov, A. Rapid Identification of Potential Inhibitors of SARS-CoV-2 Main Protease by Deep Docking of 1.3 Billion Compounds. *Mol. Inform.* **2020**, http://doi.org/10.1002/minf.202000028.
19. Zhang, L.; Lin, D.; Sun, X.; Curth, U.; Drosten, C.; Sauerhering, L.; Becker, S.; Rox, K.; Hilgenfeld, R. Crystal structure of SARS-CoV-2 main protease provides a basis for design of improved α-ketoamide inhibitors. *Science* **2020**, *368*, 409-412, http://doi.org/10.1126/science.abb3405.
20. Han, D.P.; Penn-Nicholson, A.; Cho, M.W. Identification of critical determinants on ACE2 for SARS-CoV entry and development of a potent entry inhibitor. *Virology* **2006**, *350*, 15–25, http://doi.org/10.1016/j.virol.2006.01.029.
21. Li, F.; Li, W.; Farzan, M.; Harrison, S.C. Structure of SARS coronavirus spike receptor-binding domain complexed with receptor. *Science* **2005**, *309*, 1864–8, http://doi.org/10.1126/science.1116480.
22. Souza, P.F.N.; Lopes, F.E.S.; Amaral, J.L.; Freitas, C.D.T.; Oliveira, J.T.A. A molecular docking study revealed that synthetic peptides induced conformational changes in the structure of SARS-CoV-2 spike glycoprotein, disrupting the interaction with human ACE2 receptor. *Int. J. Biol. Macromol.* **2020**, *164*, 66–76, http://doi.org/10.1016/j.ijbiomac.2020.07.174.
23. Conti, P.; Caraffa, A.; Gallenga, C.E.; Kritas, S.K.; Frydas, I.; Younes, A.; Di Emidio, P.; Tetè, G.; Pregliasco, F.; Ronconi, G. The British variant of the new coronavirus-19 (Sars-Cov-2) should not create a vaccine problem. *J Biol Regul Homeost Agents* **2021**, *35*, 1-4, http://doi.org/10.23812/21-3-e.
24. Santos, J.C.; Passos, G.A. The high infectivity of SARS-CoV-2 B.1.1.7 is associated with increased interaction force between Spike-ACE2 caused by the viral N501Y mutation. *BioRxiv* **2021**, http://doi.org/10.1101/2020.12.29.424708.
25. Luan, B.; Wang, H.; Huynh, T. Molecular Mechanism of the N501Y Mutation for Enhanced Binding between SARS-CoV-2-2's Spike Protein and Human ACE2 Receptor. *BioRxiv* **2021**, http://doi.org/10.1101/2021.01.04.425316.
26. BR, B.; Damle, H.; Ganju, S.; Damle, L. In silico screening of known small molecules to bind ACE2 specific RBD on Spike glycoprotein of SARS-CoV-2 for repurposing against COVID-19. *F1000Research* **2020**, *9*, 663, http://doi.org/10.12688/f1000research.24143.1.
27. Prajapat, M.; Shekhar, N.; Sarma, P.; Avti, P.; Singh, S.; Kaur, H.; Bhattacharyya, A.; Kumar, S.; Sharma, S.; Prakash, A.; Medhi, B. Virtual screening and molecular dynamics study of approved drugs as inhibitors of spike protein S1 domain and ACE2 interaction in SARS-CoV-2. *J. Mol. Graph. Model.* **2020**, *101*, 107716, http://doi.org/10.1016/j.jmgm.2020.107716.
28. Yan, R.; Zhang, Y.; Li, Y.; Xia, L.; Guo, Y.; Zhou, Q. Structural basis for the recognition of the SARS-CoV-2 by full-length human ACE2. *Science* **2020**, http://doi.org/10.1126/science.abb2762.

29. Tai, W.; He, L.; Zhang, X.; Pu, J.; Voronin, D.; Jiang, S.; Zhou, Y.; Du, L. Characterization of the receptor-binding domain (RBD) of 2019 novel coronavirus: implication for development of RBD protein as a viral attachment inhibitor and vaccine. *Cell. Mol. Immunol.* **2020**, http://doi.org/10.1038/s41423-020-0400-4.
30. Brooks, B.R.; Brooks, C.L.; Mackerell, A.D.; Nilsson, L.; Petrella, R.J.; Roux, B.; Won, Y.; Archontis, G.; Bartels, C.; Boresch, S.; Caflisch, A.; Caves, L.; Cui, Q.; Dinner, A.R.; Feig, M.; Fischer, S.; Gao, J.; Hodoscek, M.; Im, W., Kuczera, K.; Lazaridis, T.; Ma, J.; Ovchinnkov, V.; Paci, E.; Pastor, R.W.; Post, C.B.; Pu, J.Z.; Schaefer, M.; Tidor, B.; Venable, R.M.; Woodcock, H.L.; Wu, X.; Yang. W.; York, D.M.; Karplus, M. CHARMM: The biomolecular simulation program. *J. Comput. Chem*. **2009**, *30*, 1545–1614, http://doi.org/10.1002/jcc.21287.
31. Halgren, T.A. Merck molecular force field. I. Basis, form, scope, parameterization, and performance of MMFF94. *Journal of Computational Chemistry* **1996**, *17*, 490–519, http://doi.org/10.1002/(SICI)1096-987X(199604)17:5/6<490::AID-JCC1>3.0.CO;2-P.
32. Corporation, ChemBridge Available online: http://www.chembridge.com/screening_libraries/ (accessed on December 2020).
33. Lipinski, C.A.; Lombardo, F.; Dominy, B.W.; Feeney, P.J. Experimental and computational approaches to estimate solubility and permeability in drug discovery and development settings1PII of original article: S0169-409X(96)00423-1. The article was originally published in Advanced Drug Delivery Reviews 23 (1997) 3–25.1. *Advanced Drug Delivery Reviews* **2001**, *46*, 3-26, https://doi.org/10.1016/S0169-409X(00)00129-0.
34. Thangapandian, S.; John, S.; Lee, Y.; Kim, S.; Lee, K.W. Dynamic Structure-Based Pharmacophore Model Development: A New and Effective Addition in the Histone Deacetylase 8 (HDAC8) Inhibitor Discovery. *Int. J. Mol. Sci.* **2011**, *12*, 9440–9462, http://doi.org/10.3390/ijms12129440.
35. Vique-Sánchez, J. Potential inhibitors interacting in Neuropilin-1 to develop an adjuvant drug against COVID-19, by molecular docking. *Bioorganic & Medicinal Chemistry* **2021**, *33*, 116040, http://doi.org/10.1016/j.bmc.2021.116040.
36. Benítez-Cardoza, C.G.; Vique-Sánchez, J.L. Potential inhibitors of the interaction between ACE2 and SARS-CoV-2 (RBD), to develop a drug. *Life Sci.* **2020**, 117970, http://doi.org/10.1016/j.lfs.2020.117970.
37. Soga, S.; Shirai, H.; Kobori, M.; Hirayama, N. Use of Amino Acid Composition to Predict Ligand-Binding Sites. *J. Chem. Inf. Model*. **2007**, *47*, 400–406, http://doi.org/10.1021/ci6002202.
38. Labute, P. The generalized Born/volume integral implicit solvent model: estimation of the free energy of hydration using London dispersion instead of atomic surface area. *J. Comput. Chem*. **2008**, *29*, 1693–8, http://doi.org/10.1002/jcc.20933.
39. Wadood, A.; Ghufran, M.; Hassan, S.F.; Khan, H.; Azam, S.S.; Rashid, U. In silico identification of promiscuous scaffolds as potential inhibitors of 1-deoxy- d -xylulose 5-phosphate reductoisomerase for treatment of Falciparum malaria. *Pharmaceutical Biology* **2017**, *55*, 19–32, http://doi.org/10.1080/13880209.2016.1225778.
40. www.acdlabs.com/ Available online: https://www.acdlabs.com/products/percepta/index.php (accessed on December 2020).
41. PreADMET Available online: https://preadmet.bmdrc.kr/toxicity/ (accessed on December 2020).
42. ProTox-II Prediction of TOXicity Available online http://tox.charite.de/protox_II/index.php?site=compound_input (accessed on December 2020).
43. ADMETlab Available online: http://admet.scbdd.com/calcpre/index_sys/ (accessed on December 2020).
44. Hoffmann, M.; Kleine-Weber, H.; Schroeder, S.; Krüger, N.; Herrler, T.; Erichsen, S.; Schiergens, T.S.; Herrler, G.; Wu, N.-H.; Nitsche, A.; Muller, A.M.; Drosten, C.; Pohlmann, S. SARS-CoV-2 Cell Entry Depends on ACE2 and TMPRSS2 and Is Blocked by a Clinically Proven Protease Inhibitor. *Cell* **2020**, http://doi.org/10.1016/j.cell.2020.02.052.
45. Tai, W.; He, L.; Zhang, X.; Pu, J.; Voronin, D.; Jiang, S.; Zhou, Y.; Du, L. Characterization of the receptor-binding domain (RBD) of 2019 novel coronavirus: implication for development of RBD protein as a viral attachment inhibitor and vaccine. *Cell. Mol. Immunol.* **2020**, http://doi.org/10.1038/s41423-020-0400-4.
46. Vique-Sánchez, J.L.; Caro-Gómez, L.A.; Brieba, L.G.; Benítez-Cardoza, C.G. Developing a new drug against trichomoniasis, new inhibitory compounds of the protein triosephosphate isomerase. *Parasitol. Int.* **2020**, http://doi.org/10.1016/j.parint.2020.102086.
47. Vique-Sánchez, J.L.; Jiménez-Pineda, A.; Benítez-Cardoza, C.G. Amoebicidal effect of 5,5′-[(4-nitrophenyl)methylene]bis-6-hydroxy-2-mercapto-3-methyl-4(3 H)-pyrimidinone), a new drug against Entamoeba histolytica. *Archiv Pharmazie* **2020**, http://doi.org/10.1002/ardp.202000263.

48. Benítez-Cardoza, C.G.; Fernández-Velasco, D.A.; Vique-Sánchez, J.L. Triosephosphate Isomerase Inhibitors as Potential Drugs against Clostridium perfringens. *ChemistrySelect* **2020**, http://doi.org/10.1002/slct.201904632.
49. Arroyo-Verástegui, R.; Ortega-López, J.; Benítez-Cardoza, C.; Vique-Sánchez, L.L.; Brieba de castro, L. gabriel; Rojo-Domínguez, A.; García-Gutiérrez, P. El uso de 5,5´- [(4-nitrofenil)-metilen]bis(6-hidroxi-2-mercapto-3-metil-4(3H)-pirimidinonaTIM como tricomonicida. MX/a/2016/013109, IMPI, Mexico. **2016,** https://siga.impi.gob.mx/newSIGA/content/common/principal.jsf.

Supplementary materials

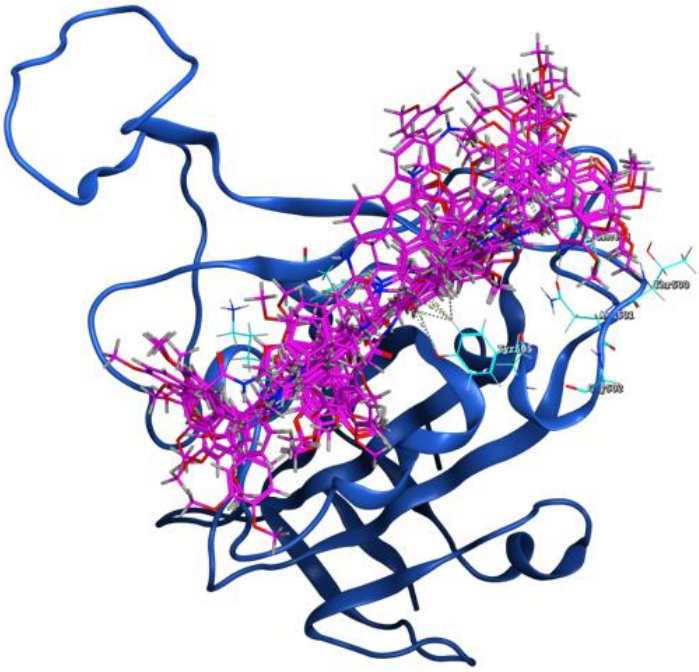

Figure S1. RBD (Blue) shows amino acids Lys417, Tyr453, Gly496, Gln498, Thr500, Gly502, and Tyr505 (Cyan), as region chosen for docking. with 25 conformers of compound R1 (Pink).

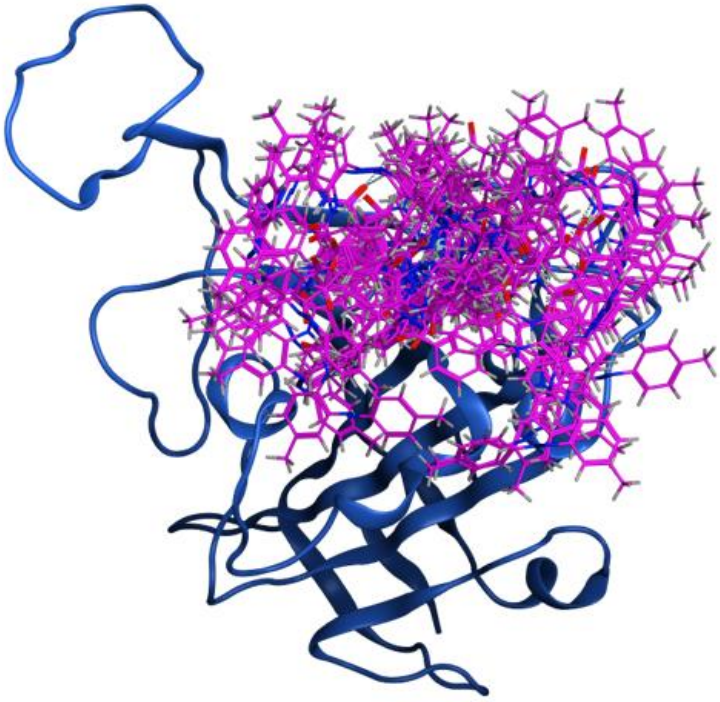

Figure S2. RBD (Blue) shows amino acids Lys417, Tyr453, Gly496, Gln498, Thr500, Gly502, and Tyr505 (Cyan), as region chosen for docking. with 28 conformers of compound R2 (Pink).

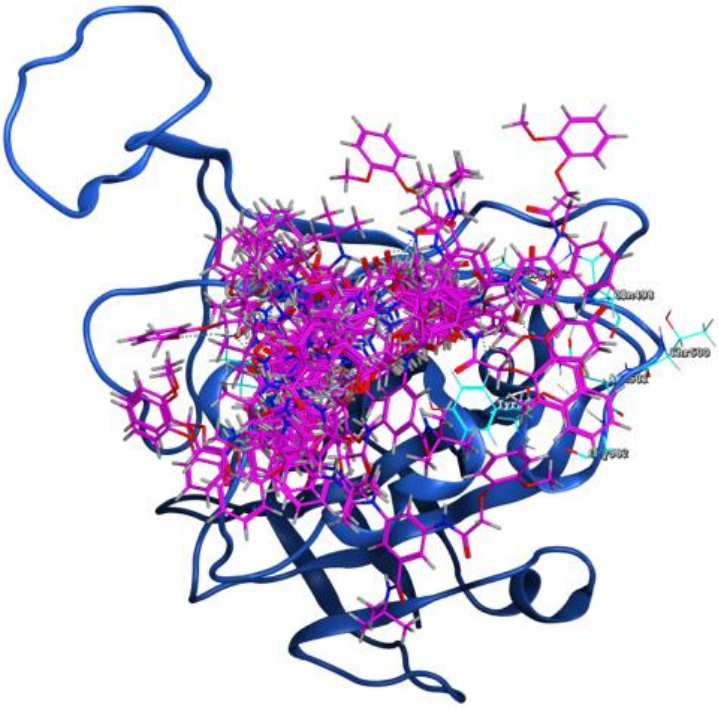

Figure S3. RBD (Blue) shows amino acids Lys417, Tyr453, Gly496, Gln498, Thr500, Gly502, and Tyr505 (Cyan), as region chosen for docking. with 23 conformers of compound R3 (Pink).

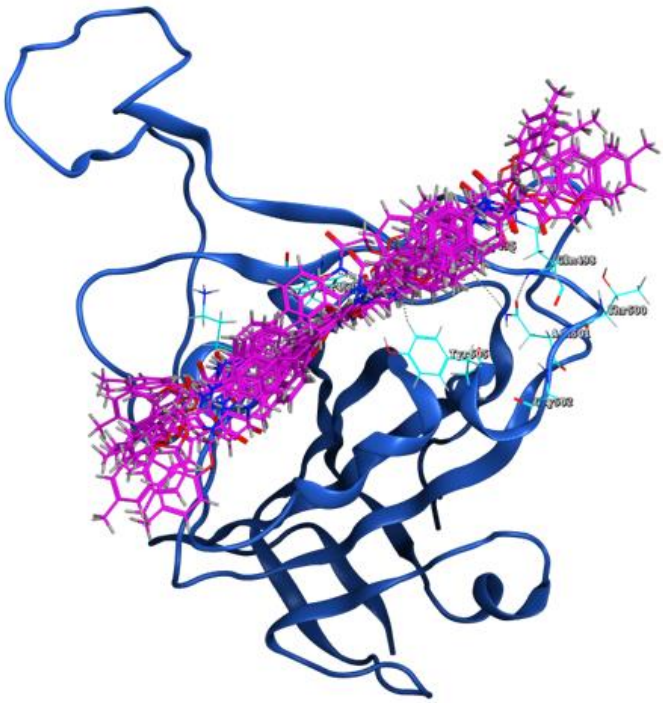

Figure S4. RBD (Blue) shows amino acids Lys417, Tyr453, Gly496, Gln498, Thr500, Gly502, and Tyr505 (Cyan), as region chosen for docking. with 23 conformers of compound R4 (Pink).

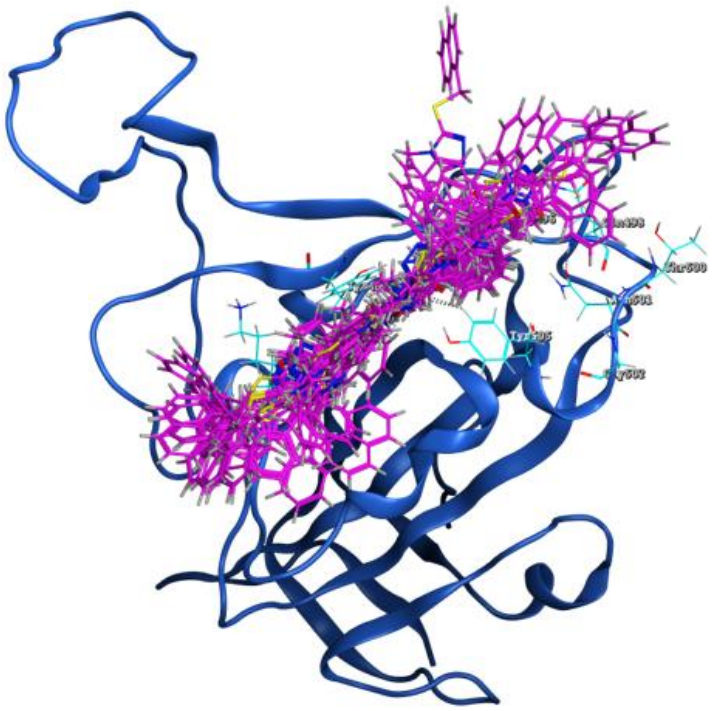

Figure S5. RBD (Blue) shows amino acids Lys417, Tyr453, Gly496, Gln498, Thr500, Gly502, and Tyr505 (Cyan), as region chosen for docking. with 27 conformers of compound R5 (Pink).

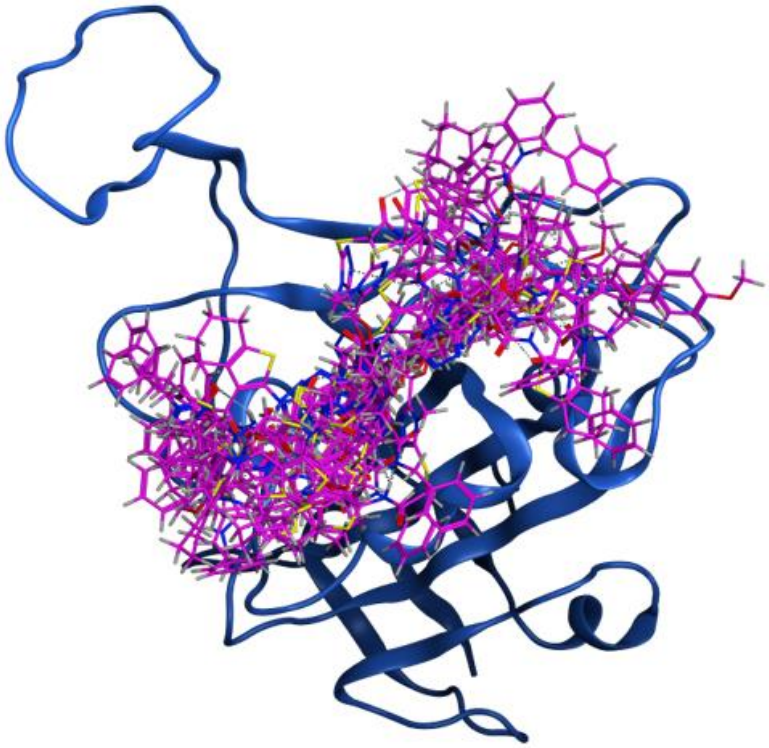

Figure S6. RBD (Blue) shows amino acids Lys417, Tyr453, Gly496, Gln498, Thr500, Gly502, and Tyr505 (Cyan), as region chosen for docking. with 26 conformers of compound R6 (Pink).

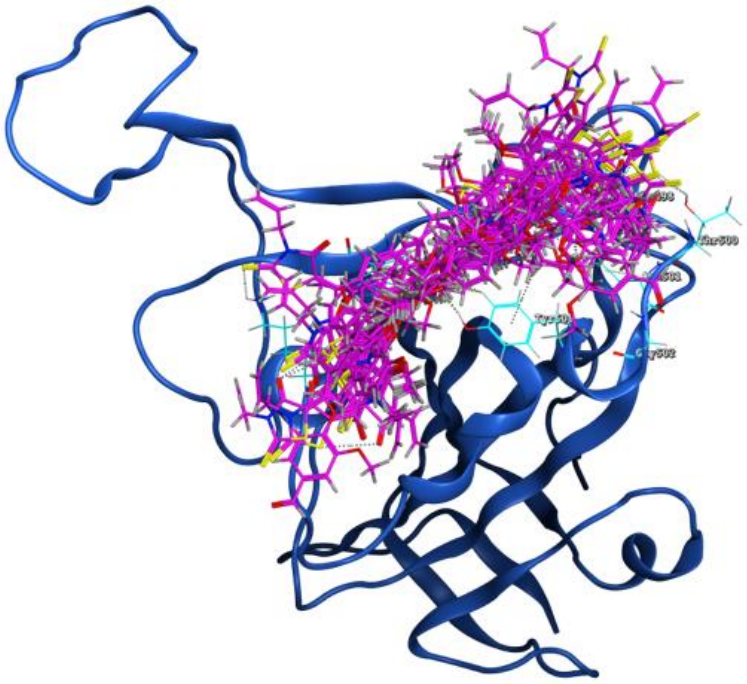

Figure S7. RBD (Blue) shows amino acids Lys417, Tyr453, Gly496, Gln498, Thr500, Gly502, and Tyr505 (Cyan), as region chosen for docking. with 26 conformers of compound R7 (Pink).

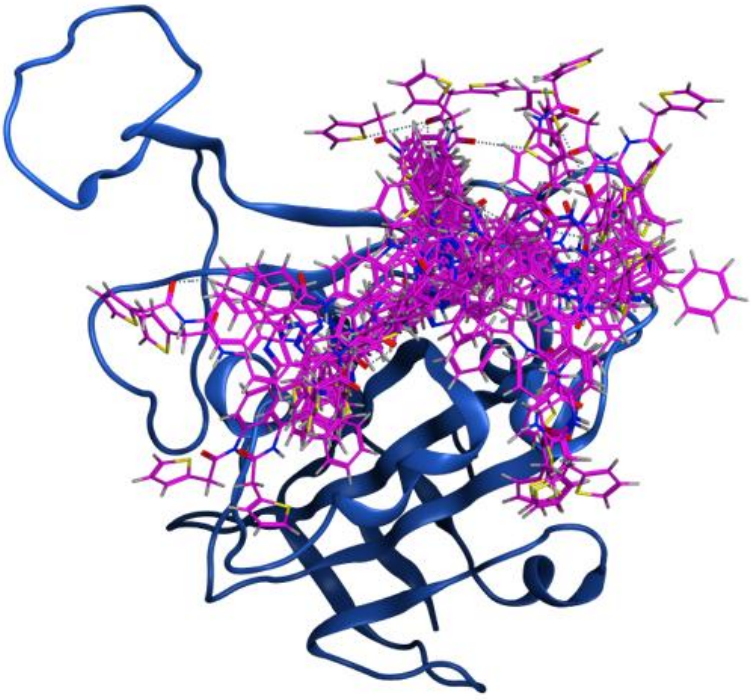

Figure S8. RBD (Blue) shows amino acids Lys417, Tyr453, Gly496, Gln498, Thr500, Gly502, and Tyr505 (Cyan), as region chosen for docking. with 25 conformers of compound R8 (Pink).

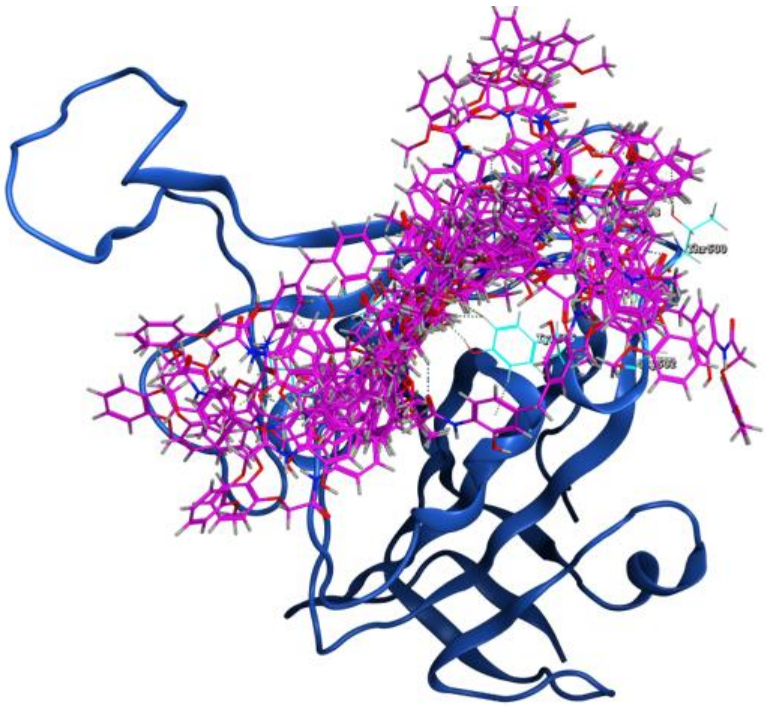

Figure S9. RBD (Blue) shows amino acids Lys417, Tyr453, Gly496, Gln498, Thr500, Gly502, and Tyr505 (Cyan), as region chosen for docking. with 30 conformers of compound R9 (Pink).

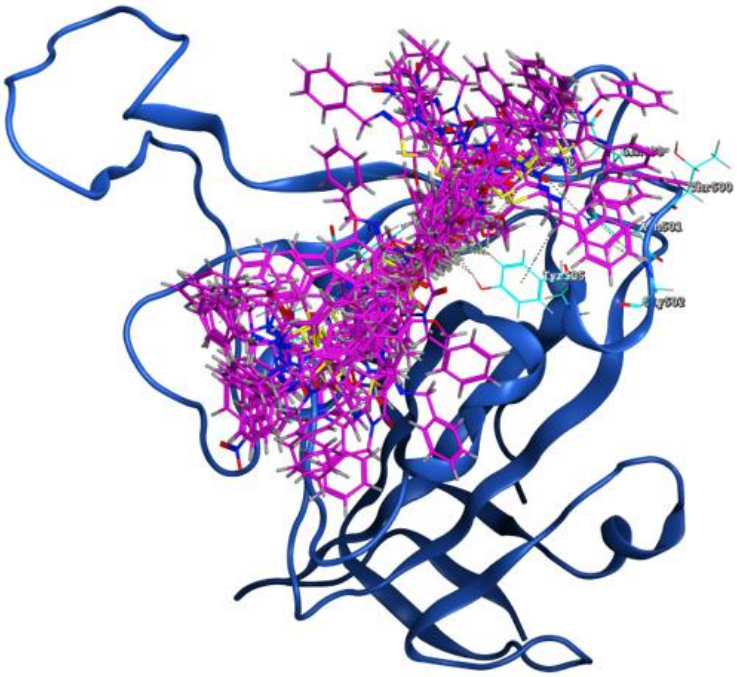

Figure S10. RBD (Blue) shows amino acids Lys417, Tyr453, Gly496, Gln498, Thr500, Gly502, and Tyr505 (Cyan), as region chosen for docking with 26 conformers of compound R10 (Pink).

Table S1. $\Delta G_{binding}$ of conformers (23 to 30 conformers) of each compound. Determining the average and SD.

Compound	Conformer	ΔGbinding
R1	1	-7.2331119
R1	2	-7.2060246
R1	3	-7.0339036
R1	4	-6.8647242
R1	5	-6.7495556
R1	6	-6.7483559

Compound	Conformer	ΔGbinding
R1	7	-6.6875863
R1	8	-6.4959726
R1	9	-6.4462318
R1	10	-6.4292998
R1	11	-6.3906956
R1	12	-6.3088284
R1	13	-6.2796907
R1	14	-6.2491703
R1	15	-6.158937
R1	16	-6.109056
R1	17	-6.0130754
R1	18	-5.9979191
R1	19	-5.9444871
R1	20	-5.857439
R1	21	-5.6574349
R1	22	-5.3348861
R1	23	-5.1818366
R1	24	-5.1590252
R1	25	-4.8872619
	Average $\Delta G_{binding}$	-6.21698038
	SD	± 0.62
R2	1	-6.7664809
R2	2	-6.4214549
R2	3	-6.3933887
R2	4	-6.3315854
R2	5	-6.32091
R2	6	-6.3154831
R2	7	-6.314508
R2	8	-6.2792678
R2	9	-6.2149229
R2	10	-6.2144265
R2	11	-6.1770554
R2	12	-6.1106873
R2	13	-6.1036081
R2	14	-6.0555568
R2	15	-6.0159683
R2	16	-5.9760051
R2	17	-5.8339138
R2	18	-5.8242407
R2	19	-5.693037
R2	20	-5.6349249
R2	21	-5.631999
R2	22	-5.5930738
R2	23	-5.5459528
R2	24	-5.5203071
R2	25	-5.351244
R2	26	-5.2036734
R2	27	-5.1064463
R2	28	-4.791348
	Average $\Delta G_{binding}$	-5.91933821
	SD	± 0.46
R3	1	-6.9838405
R3	2	-6.8462219
R3	3	-6.8056817
R3	4	-6.5285497
R3	5	-6.1570921

Compound	Conformer	ΔGbinding
R3	6	-6.1317654
R3	7	-6.1204648
R3	8	-6.0225105
R3	9	-6.0142112
R3	10	-5.9668207
R3	11	-5.9426217
R3	12	-5.9286957
R3	13	-5.9193277
R3	14	-5.880055
R3	15	-5.712388
R3	16	-5.6240087
R3	17	-5.5277014
R3	18	-5.5202971
R3	19	-5.4840665
R3	20	-5.4422593
R3	21	-5.1444192
R3	22	-4.9145379
R3	23	-4.7276583
	Average $\Delta G_{binding}$	-5.8845737
	SD	± 0.57
R4	1	-6.7632031
R4	2	-6.4043522
R4	3	-6.2631483
R4	4	-6.2200856
R4	5	-6.1751533
R4	6	-6.1260304
R4	7	-6.1187668
R4	8	-6.0734396
R4	9	-5.996778
R4	10	-5.9447236
R4	11	-5.9102702
R4	12	-5.8583083
R4	13	-5.8441443
R4	14	-5.8113565
R4	15	-5.7965097
R4	16	-5.6938453
R4	17	-5.5749726
R4	18	-5.5663042
R4	19	-5.5587106
R4	20	-5.5300426
R4	21	-5.5095415
R4	22	-5.1574287
R4	23	-4.55792
	Average $\Delta G_{binding}$	-5.8458711
	SD	± 0.44
R5	1	-7.0540476
R5	2	-6.9974627
R5	3	-6.7864766
R5	4	-6.5201869
R5	5	-6.3118415
R5	6	-6.1991568
R5	7	-6.1128678
R5	8	-5.9717464
R5	9	-5.9277887
R5	10	-5.9091444
R5	11	-5.8888454

Compound	Conformer	ΔGbinding
R5	12	-5.7561822
R5	13	-5.7483029
R5	14	-5.7370377
R5	15	-5.7046599
R5	16	-5.609766
R5	17	-5.609632
R5	18	-5.5986104
R5	19	-5.5095038
R5	20	-5.4846411
R5	21	-5.4378185
R5	22	-5.4288836
R5	23	-5.4227753
R5	24	-5.2630024
R5	25	-5.2263398
R5	26	-5.1524119
R5	27	-5.1467886
	Average $\Delta G_{binding}$	-5.833923
	SD	± 0.52
R6	1	-6.6316271
R6	2	-6.531496
R6	3	-6.3979082
R6	4	-6.3553157
R6	5	-6.1730232
R6	6	-6.1443419
R6	7	-6.0652223
R6	8	-6.0623302
R6	9	-6.0476213
R6	10	-6.013927
R6	11	-5.9997869
R6	12	-5.9780679
R6	13	-5.9647527
R6	14	-5.9493237
R6	15	-5.9476452
R6	16	-5.8769274
R6	17	-5.7677441
R6	18	-5.7652736
R6	19	-5.6708832
R6	20	-5.6249809
R6	21	-5.6151843
R6	22	-5.5595589
R6	23	-5.4790697
R6	24	-5.4070182
R6	25	-5.3746576
R6	26	-5.0022559
R6	27	-5.0015974
R6	28	-4.9277129
	Average $\Delta G_{binding}$	-5.83340191
	SD	0.43583264
R7	1	-6.8522887
R7	2	-6.5122266
R7	3	-6.4491115
R7	4	-6.4435782
R7	5	-6.4315424
R7	6	-6.1583447
R7	7	-6.0595407
R7	8	-6.0270767

Compound	Conformer	ΔGbinding
R7	9	-6.0180469
R7	10	-6.0068564
R7	11	-5.9803696
R7	12	-5.8949351
R7	13	-5.8882146
R7	14	-5.8428049
R7	15	-5.8407564
R7	16	-5.8271775
R7	17	-5.745029
R7	18	-5.5404458
R7	19	-5.5223618
R7	20	-5.4813976
R7	21	-5.4163742
R7	22	-5.3106384
R7	23	-5.2996225
R7	24	-5.2951803
R7	25	-5.1050701
R7	26	-4.701251
	Average $\Delta G_{binding}$	-5.8327016
	SD	± 0.6249
R8	1	-6.7326531
R8	2	-6.5280132
R8	3	-6.523767
R8	4	-6.503541
R8	5	-6.0592937
R8	6	-6.0208974
R8	7	-6.0082111
R8	8	-5.9772091
R8	9	-5.8727155
R8	10	-5.8443942
R8	11	-5.8211112
R8	12	-5.817112
R8	13	-5.7668514
R8	14	-5.7560153
R8	15	-5.7452903
R8	16	-5.6895194
R8	17	-5.680151
R8	18	-5.6375241
R8	19	-5.6060319
R8	20	-5.5317001
R8	21	-5.5244312
R8	22	-5.4838753
R8	23	-5.3497686
R8	24	-5.0877872
R8	25	-5.0507255
	Average $\Delta G_{binding}$	-5.82474359
	SD	0.41922409
R9	1	-6.6013284
R9	2	-6.6013021
R9	3	-6.54562
R9	4	-6.3383489
R9	5	-6.3168378
R9	6	-6.3073845
R9	7	-6.272552
R9	8	-6.1454167
R9	9	-6.1359248

Compound	Conformer	ΔGbinding
R9	10	-6.1313753
R9	11	-6.0432882
R9	12	-5.9264412
R9	13	-5.9164457
R9	14	-5.8949504
R9	15	-5.8537846
R9	16	-5.8511791
R9	17	-5.8180528
R9	18	-5.7812982
R9	19	-5.758338
R9	20	-5.73105
R9	21	-5.702023
R9	22	-5.6906929
R9	23	-5.6595364
R9	24	-5.5401473
R9	25	-5.5328937
R9	26	-5.512238
R9	27	-5.3337536
R9	28	-5.0034127
R9	29	-4.8866568
R9	30	-3.7863204
	Average $\Delta G_{binding}$	-5.82061978
	SD	± 0.56
R10	1	-6.7684965
R10	2	-6.7468953
R10	3	-6.6069436
R10	4	-6.3902907
R10	5	-6.3285928
R10	6	-6.0805092
R10	7	-6.0715919
R10	8	-6.0187011
R10	9	-5.9624271
R10	10	-5.8690481
R10	11	-5.8441906
R10	12	-5.8227491
R10	13	-5.8006115
R10	14	-5.7594738
R10	15	-5.7442722
R10	16	-5.7260971
R10	17	-5.7088141
R10	18	-5.6658616
R10	19	-5.5842304
R10	20	-5.5423489
R10	21	-5.4113111
R10	22	-5.2722654
R10	23	-5.197022
R10	24	-5.1839638
R10	25	-5.1252923
R10	26	-5.0220327
R10	Average $\Delta G_{binding}$	-5.8174628
	SD	± 0.47

Table S2. Interaction report of each conformer of compound R1. Number of conformer, Atom of compound, Residue in RBD, Type of interaction and Distance in angstroms.

Conformer	**Ligand**	**Residues in RBD**		**Interaction**	**Distance**
1	O	LYS	417	H-acceptor	3.12
2	O	LYS	417	H-acceptor	3.12

3	N	GLU	406	H-donor	3.34
4	O	LYS	417	H-acceptor	3.07
5	O	LYS	417	H-acceptor	3.11
	6-ring	GLY	416	pi-H	4.01
6	6-ring	GLY	496	pi-H	3.63
7	N	GLU	406	H-donor	3.36
	6-ring	TYR	505	pi-H	4.37
	6-ring	TYR	505	pi-H	4.45
8	N	GLU	406	H-donor	3.36
	6-ring	TYR	505	pi-H	4.52
	6-ring	TYR	505	pi-H	4.38
9	O	LYS	417	H-acceptor	3.34
	6-ring	GLY	416	pi-H	4
10	N	GLU	406	H-donor	3.39
11	6-ring	TYR	505	pi-H	3.98
12	6-ring	GLN	498	pi-H	3.96
13	6-ring	GLY	496	pi-H	3.82
14	6-ring	GLN	498	pi-H	3.91
15	6-ring	GLN	498	pi-H	3.85
	6-ring	TYR	505	pi-H	3.74
16	6-ring	TYR	505	pi-H	4.01
	6-ring	TYR	505	pi-H	4.41
17	6-ring	GLY	416	pi-H	4.1
18	O	TYR	505	H-acceptor	3.32
19	O	ARG	403	H-acceptor	3.08
	6-ring	TYR	505	pi-H	4.02
20	O	TYR	449	H-acceptor	3

Table S3. Interaction report of each conformer of compound R2. Number of conformer, Atom of compound, Residue in RBD, Type of interaction and Distance in angstroms.

Conformer	**Ligand**	**Residues in RBD**		**Interaction**	**Distance**
1	6-ring	LYS	417	pi-H	3.97
2	O	TYR	453	H-acceptor	2.87
	6-ring	TYR	449	pi-H	3.57
	6-ring	GLY	496	pi-H	3.79
3	6-ring	PHE	456	pi-H	4.09
4	6-ring	GLY	502	pi-H	4.1
5	6-ring	GLY	496	pi-H	4.57
6	O	TYR	453	H-acceptor	2.88
	6-ring	TYR	449	pi-H	3.61
7	6-ring	TYR	449	pi-H	4.63
8	O	GLY	502	H-acceptor	3.03
	6-ring	GLY	496	pi-H	3.84
	6-ring	TYR	505	pi-H	3.88
9	O	TYR	449	H-acceptor	2.79
	6-ring	TYR	453	pi-H	3.42
	6-ring	GLN	498	pi-H	4.67
10	6-ring	TYR	495	pi-H	4.83
	6-ring	THR	500	pi-H	3.95
11	N	GLN	493	H-acceptor	3.29
12	6-ring	PHE	456	pi-H	4.16
13	6-ring	GLY	496	pi-H	3.67
	6-ring	GLN	498	pi-H	4.3
14	6-ring	GLY	496	pi-H	3.77
15	6-ring	TYR	495	pi-H	4.85
16	6-ring	GLY	502	pi-H	4.05
	6-ring	TYR	505	pi-H	3.87
	6-ring	TYR	505	pi-pi	3.9

Conformer	Ligand	Residues in RBD		Interaction	Distance
17	6-ring	TYR	449	pi-H	3.8
	6-ring	LEU	455	pi-H	4.1
18	O	GLY	496	H-acceptor	3.24
19	N	GLY	502	H-acceptor	3.14
	6-ring	GLN	498	pi-H	4.02
20	6-ring	GLN	493	pi-H	3.79
	6-ring	TYR	495	pi-H	4.77

Table S4. Interaction report of each conformer of compound R3. Number of conformer, Atom of compound, Residue in RBD, Type of interaction and Distance in angstroms.

Conformer	Ligand	Residues in RBD		Interaction	Distance
1	O	LYS	417	H-acceptor	3.16
2	O	GLN	493	H-acceptor	3.29
	O	LYS	417	H-acceptor	3.4
	6-ring	GLY	496	pi-H	3.83
3	6-ring	LYS	417	pi-H	4.16
4	6-ring	LYS	417	pi-H	4.29
	6-ring	GLY	496	pi-H	3.75
5	O	ARG	403	H-acceptor	2.97
6	O	ARG	403	H-acceptor	3.09
7	O	ARG	403	H-acceptor	3.05
	6-ring	GLY	416	pi-H	4.17
9	O	LYS	417	H-acceptor	2.93
	O	ARG	403	H-acceptor	2.91
	6-ring	TYR	495	pi-H	4.78
10	O	ARG	403	H-acceptor	3.12
11	O	LYS	417	H-acceptor	3.18
12	O	ARG	403	H-acceptor	2.94
	6-ring	TYR	495	pi-H	4.78
13	O	ARG	408	H-acceptor	2.87
14	O	ARG	403	H-acceptor	2.89
15	O	LYS	417	H-acceptor	3.22
16	6-ring	GLY	502	pi-H	4.93
17	O	LYS	417	H-acceptor	3.16
18	O	ARG	408	H-acceptor	3.14
	O	ARG	408	H-acceptor	3.41
	6-ring	ARG	403	pi-cation	3.95

Table S5. Interaction report of each conformer of compound R4. Number of conformer, Atom of compound, Residue in RBD, Type of interaction and Distance in angstroms.

Conformer	Ligand	Residues in RBD		Interaction	Distance
1	6-ring	THR	415	pi-H	3.86
	6-ring	LYS	417	pi-H	4.39
	6-ring	GLY	496	pi-H	4.07
2	6-ring	THR	415	pi-H	3.86
	6-ring	LYS	417	pi-H	4.84
	6-ring	GLY	496	pi-H	3.86
3	O	TYR	449	H-acceptor	2.96
4	6-ring	LYS	417	pi-H	4.24
5	N	GLU	406	H-donor	3.41
	6-ring	LYS	417	pi-H	4.21
	6-ring	GLY	496	pi-H	4.41
6	6-ring	GLY	496	pi-H	3.92

Conformer	Ligand	Residues in RBD		Interaction	Distance
7	6-ring	GLY	446	pi-H	3.93
8	O	LYS	417	H-acceptor	3.37
	6-ring	GLY	496	pi-H	3.92
9	6-ring	THR	415	pi-H	3.92
10	O	TYR	453	H-acceptor	3.04
11	O	LYS	417	H-acceptor	3.23
	6-ring	GLY	496	pi-H	4.04
12	6-ring	GLY	446	pi-H	3.84
13	6-ring	GLY	496	pi-H	4
14	O	LYS	417	H-acceptor	3.33
15	O	TYR	453	H-acceptor	3.12
	6-ring	ARG	403	pi-cation	3.77
	6-ring	THR	415	pi-H	4.01

Table S6. Interaction report of each conformer of compound R5. Number of conformer, Atom of compound, Residue in RBD, Type of interaction and Distance in angstroms.

Conformer	Ligand	Residues in RBD		Interaction	Distance
1	N	GLU	406	H-donor	3.43
	6-ring	GLY	496	pi-H	3.71
2	N	GLU	406	H-donor	3.36
	6-ring	GLY	496	pi-H	3.78
3	N	GLU	406	H-donor	3.39
	6-ring	GLY	496	pi-H	3.73
4	N	GLU	406	H-donor	3.32
	N	LYS	417	H-donor	3.08
5	5-ring	LYS	417	pi-H	3.78
6	5-ring	LYS	417	pi-H	3.85
	6-ring	GLY	496	pi-H	3.95
7	6-ring	LYS	417	pi-H	4.4
	6-ring	GLN	498	pi-H	3.89
8	6-ring	GLY	416	pi-H	4.32
9	5-ring	ARG	403	pi-cation	4.14
	6-ring	ARG	408	pi-cation	3.77
10	6-ring	GLY	496	pi-H	3.64
11	6-ring	ARG	403	pi-cation	3.48
12	6-ring	GLY	416	pi-H	3.98
13	O	LYS	417	H-acceptor	3.24
	6-ring	GLY	496	pi-H	3.62
14	6-ring	GLY	496	pi-H	4
15	N	GLY	496	H-donor	3.27
16	O	GLY	496	H-acceptor	3.54
17	6-ring	GLY	416	pi-H	3.89
18	6-ring	GLY	496	pi-H	3.67
19	O	GLY	496	H-acceptor	3.51
20	6-ring	GLY	446	pi-H	4.61
21	O	LYS	417	H-acceptor	3.09
	6-ring	GLY	496	pi-H	3.68
22	6-ring	ARG	403	pi-cation	3.55
23	6-ring	ARG	403	pi-cation	3.63
	6-ring	ARG	403	pi-cation	4.09
24	N	TYR	449	H-donor	3.11

Table S7. Interaction report of each conformer of compound R6. Number of conformer, Atom of compound, Residue in RBD, Type of interaction and Distance in angstroms.

Conformer	**Ligand**	**Residues in RBD**		**Interaction**	**Distance**
1	5-ring	LYS	417	pi-H	4.61
2	C	TYR	505	H-pi	4.13
3	5-ring	TYR	505	pi-H	4.45
4	6-ring	GLY	416	pi-H	4.01
	6-ring	TYR	505	pi-H	3.81
5	5-ring	LYS	417	pi-H	4.22
	6-ring	TYR	505	pi-H	4.22
6	6-ring	GLY	416	pi-H	3.96
7	6-ring	ASN	460	pi-H	3.61
	6-ring	TYR	505	pi-H	4.35
8	5-ring	LYS	417	pi-H	4.19
	6-ring	TYR	505	pi-H	4.19
9	O	ARG	408	H-acceptor	2.96
	5-ring	ARG	403	pi-cation	3.57
10	5-ring	LYS	417	pi-H	4.64
11	S	GLN	493	H-donor	3.66
	5-ring	TYR	505	pi-H	4.2
12	5-ring	ARG	403	pi-cation	3.45
13	6-ring	TYR	453	pi-H	3.58
14	5-ring	ARG	403	pi-cation	4.04
15	O	ARG	403	H-acceptor	2.94
16	N	ARG	403	H-acceptor	3.04
17	N	GLN	493	H-acceptor	3.24
	N	GLN	493	H-acceptor	3.21
	6-ring	TYR	505	pi-H	3.88
18	S	SER	494	H-donor	3.6
	O	TYR	449	H-acceptor	3
	5-ring	TYR	453	pi-H	4.28

Table S8. Interaction report of each conformer of compound R7. Number of conformer, Atom of compound, Residue in RBD, Type of interaction and Distance in angstroms.

Conformer	**Ligand**	**Residues in RBD**		**Interaction**	**Distance**
1	S	ARG	408	H-acceptor	3.6
	O	ARG	403	H-acceptor	2.87
	6-ring	GLY	496	pi-H	4.07
2	S	ARG	408	H-acceptor	3.68
	O	ARG	403	H-acceptor	2.88
	6-ring	GLY	496	pi-H	4.16
3	S	ARG	408	H-acceptor	3.65
	O	ARG	403	H-acceptor	2.83
	6-ring	GLY	496	pi-H	4.16
4	S	ARG	408	H-acceptor	3.71
	O	ARG	403	H-acceptor	2.81
	6-ring	GLY	496	pi-H	4.13
5	O	ARG	408	H-acceptor	3.03
6	O	ARG	408	H-acceptor	3.01
	C	TYR	505	pi-H	4.57
7	5-ring	GLY	416	pi-H	3.78
8	O	ARG	408	H-acceptor	3.17
	5-ring	GLN	498	pi-H	3.88
9	6-ring	GLY	496	pi-H	4.13
10	6-ring	GLY	496	pi-H	3.95
11	O	GLN	498	H-acceptor	3.24
	5-ring	GLY	416	pi-H	3.98
12	6-ring	GLY	496	pi-H	3.92

Conformer	**Ligand**	**Residues in RBD**		**Interaction**	**Distance**
13	O	LYS	417	H-acceptor	3.19
14	O	ARG	408	H-acceptor	3.04
15	5-ring	GLY	446	pi-H	4.45
	6-ring	GLY	496	pi-H	4.29
16	6-ring	TYR	505	pi-H	4.17
	6-ring	TYR	505	pi-H	4.04
17	S	THR	500	H-acceptor	4.32
	5-ring	GLN	498	pi-H	3.9
18	5-ring	GLN	498	pi-H	3.95
19	S	THR	500	H-acceptor	3.82
	O	LYS	417	H-acceptor	3.02
	5-ring	GLN	498	pi-H	3.78
	6-ring	TYR	505	pi-H	3.52
20	S	LYS	417	H-acceptor	3.79
	O	ARG	403	H-acceptor	3
21	6-ring	GLY	496	pi-H	4.11
22	S	TYR	449	H-acceptor	4.28
	S	GLN	498	H-acceptor	4.39
23	S	LYS	417	H-acceptor	4.2

Table S9. Interaction report of each conformer of compound R8. Number of conformer, Atom of compound, Residue in RBD, Type of interaction and Distance in angstroms.

Conformer	**Ligand**	**Residues in RBD**		**Interaction**	**Distance**
1	6-ring	GLY	496	pi-H	3.65
2	S	GLU	406	H-donor	3.71
	6-ring	TYR	449	pi-H	4.57
3	N	GLU	406	H-donor	3.33
	6-ring	TYR	449	pi-H	4.54
4	S	GLU	406	H-donor	3.98
	N	GLU	406	H-donor	3.32
	6-ring	TYR	449	pi-H	4.63
5	N	ARG	403	H-acceptor	3.2
	O	LYS	417	H-acceptor	3.26
6	6-ring	GLN	498	pi-H	4.09
	5-ring	GLY	504	pi-H	4.1
7	6-ring	GLY	496	pi-H	3.53
8	N	GLU	406	H-donor	3.19
9	O	TYR	453	H-acceptor	3.09
	6-ring	GLY	496	pi-H	3.86
10	S	GLN	409	H-donor	3.94
	S	GLY	502	H-donor	3.55
	O	ARG	403	H-acceptor	3.43
11	S	GLU	406	H-donor	4.07
	N	GLU	406	H-donor	3.23
12	S	GLU	406	H-donor	3.96
13	6-ring	THR	500	pi-H	3.88
14	6-ring	LYS	417	pi-cation	4.58
15	6-ring	GLN	498	pi-H	4.49
	5-ring	GLY	504	pi-H	4.2
16	O	ARG	403	H-acceptor	2.9
17	O	GLY	496	H-acceptor	3.37
	6-ring	GLN	498	pi-H	3.7
18	S	ASP	420	H-donor	3.7
	5-ring	THR	415	pi-H	4.44
19	O	TYR	449	H-acceptor	3.05
	6-ring	GLY	502	pi-H	3.93
20	6-ring	TYR	505	pi-H	4.17

Table S10. Interaction report of each conformer of compound R9. Number of conformer, Atom of compound, Residue in RBD, Type of interaction and Distance in angstroms.

Conformer	**Ligand**	**Residues in RBD**		**Interaction**	**Distance**
1	O	GLY	496	H-donor	3.04
2	6-ring	ALA	475	pi-H	4.3
3	O	SER	494	H-donor	2.97
	O	ARG	403	H-acceptor	3.17
	6-ring	TYR	505	pi-H	3.88
4	6-ring	LYS	417	pi-H	4.33
5	6-ring	TYR	495	pi-H	4.4
6	6-ring	TYR	505	pi-H	4.13
7	6-ring	ARG	403	pi-cation	3.47
8	O	GLY	496	H-donor	3.12
	6-ring	GLY	502	pi-H	3.96
9	O	SER	494	H-donor	2.9
	O	GLY	496	H-donor	3.01
	6-ring	THR	500	pi-H	3.61
10	O	GLY	502	H-acceptor	3.44
	6-ring	TYR	505	pi-H	4
11	O	GLY	496	H-acceptor	3.16
12	6-ring	LYS	417	pi-H	4.13
13	O	ARG	403	H-acceptor	2.95
	6-ring	TYR	453	pi-H	3.38
14	O	GLY	496	H-acceptor	3.15
15	O	SER	494	H-donor	3.06
	O	GLY	496	H-donor	3
	O	TYR	505	H-acceptor	3.06
	6-ring	THR	500	pi-H	3.54
16	O	GLY	496	H-acceptor	3.19
	6-ring	GLY	502	pi-H	4.02
17	O	GLY	496	H-acceptor	3.12
18	6-ring	ARG	403	pi-cation	3.87
	6-ring	THR	500	pi-H	3.73
19	O	GLY	496	H-donor	3.18
	6-ring	ARG	403	pi-cation	3.86
	6-ring	THR	500	pi-H	3.67
20	6-ring	ARG	403	pi-cation	3.71
	6-ring	LYS	417	pi-H	4.22
21	6-ring	ARG	403	pi-cation	3.59
	6-ring	TYR	449	pi-H	3.61
22	O	ARG	403	H-acceptor	3.05
	6-ring	GLY	502	pi-H	3.74
23	O	GLY	496	H-acceptor	3.22
24	6-ring	ARG	403	pi-cation	3.56

Table S11. Interaction report of each conformer of compound R10. Number of conformer, Atom of compound, Residue in RBD, Type of interaction and Distance in angstroms.

Conformer	**Ligand**	**Residues in RBD**		**Interaction**	**Distance**
1	6-ring	ARG	408	pi-cation	3.97
	6-ring	ARG	408	pi-cation	4.48
	6-ring	GLY	496	pi-H	3.9
2	O	TYR	449	H-acceptor	2.82
3	O	ASN	460	H-acceptor	3.11
	6-ring	GLY	416	pi-H	3.99
	6-ring	TYR	453	pi-H	3.7
4	O	LYS	417	H-acceptor	3.37
	5-ring	LYS	417	pi-H	4.23
	6-ring	LYS	417	pi-cation	3.68

Conformer	Ligand	Residues in RBD		Interaction	Distance
5	O	ARG	403	H-acceptor	3.16
6	O	GLY	496	H-acceptor	3.48
	5-ring	LYS	417	pi-H	4.32
	6-ring	LYS	417	pi-cation	4.68
7	O	GLY	496	H-acceptor	3.15
	5-ring	LYS	417	pi-H	4.12
	6-ring	LYS	417	pi-cation	4.11
8	O	TYR	449	H-acceptor	3.02
9	O	GLN	409	H-acceptor	3.18
	O	LYS	417	H-acceptor	3.31
	6-ring	TYR	505	pi-H	3.94
10	5-ring	LYS	417	pi-H	4.39
	6-ring	LYS	417	pi-cation	4.71
	6-ring	TYR	505	pi-H	4.18
11	O	GLY	496	H-acceptor	3.25
12	O	GLY	496	H-acceptor	3.14
	5-ring	LYS	417	pi-H	4.32
	6-ring	LYS	417	pi-cation	3.96
13	6-ring	GLY	502	pi-H	4.7
14	O	TYR	449	H-acceptor	2.87
15	O	ARG	403	H-acceptor	3.43
16	C	TYR	505	H-acceptor	4.51
	6-ring	GLY	502	pi-H	4.24
	6-ring	TYR	505	pi-H	4.59
17	6-ring	GLY	416	pi-H	3.86
	5-ring	LYS	417	pi-H	4.19
18	6-ring	ARG	403	pi-cation	3.69
19	6-ring	ARG	403	pi-cation	3.67
20	6-ring	ARG	403	pi-cation	4.51
	6-ring	TYR	505	pi-H	3.69
21	6-ring	TYR	505	pi-H	4.13
22	O	ARG	408	H-acceptor	2.96
	6-ring	ARG	403	pi-cation	3.86

Table S12. Toxicity – PreADMET | Prediction of ADME/Tox of compounds R1–R10.

R1.-		**R2.-**	
algae_at	0.00214501	algae_at	0.000109963
Ames_test	mutagen	Ames_test	mutagen
Carcino_Mouse	negative	Carcino_Mouse	negative
Carcino_Rat	positive	Carcino_Rat	positive
daphnia_at	0.00325711	daphnia_at	5.33816e-005
hERG_inhibition	medium_risk	hERG_inhibition	medium_risk
medaka_at	3.60617e-005	medaka_at	1.39616e-008
minnow_at	0.000448392	minnow_at	5.4765e-008
TA100_10RLI	negative	TA100_10RLI	positive
TA100_NA	negative	TA100_NA	negative
TA1535_10RLI	negative	TA1535_10RLI	negative
TA1535_NA	negative	TA1535_NA	negative
R3.-		**R4.-**	
algae_at	0.00455501	algae_at	0.00499145
Ames_test	non-mutagen	Ames_test	non-mutagen
Carcino_Mouse	negative	Carcino_Mouse	positive
Carcino_Rat	negative	Carcino_Rat	negative
daphnia_at	0.0293256	daphnia_at	0.00143501
hERG_inhibition	ambiguous	hERG_inhibition	medium_risk
medaka_at	0.00227046	medaka_at	7.03412e-006
minnow_at	0.00656983	minnow_at	0.000295601
TA100_10RLI	negative	TA100_10RLI	negative
TA100_NA	negative	TA100_NA	negative

TA1535_10RLI	negative
TA1535_NA	negative
R5.-	
algae_at	0.00332662
Ames_test mutagen	
Carcino_Mouse	positive
Carcino_Rat	negative
daphnia_at	0.00101714
hERG_inhibition	medium_risk
medaka_at	4.33827e-006
minnow_at	9.19423e-005
TA100_10RLI	negative
TA100_NA	negative
TA1535_10RLI	negative
TA1535_NA	negative
R7.-	
algae_at	0.00216639
Ames_test mutagen	
Carcino_Mouse	negative
Carcino_Rat	negative
daphnia_at	0.000262349
hERG_inhibition	medium_risk
medaka_at	3.68939e-007
minnow_at	9.96095e-007
TA100_10RLI	negative
TA100_NA	negative
TA1535_10RLI	negative
TA1535_NA	negative
R9.-	
algae_at	0.00303018
Ames_test non-mutagen	
Carcino_Mouse	negative
Carcino_Rat	negative
daphnia_at	0.00393424
hERG_inhibition	ambiguous
medaka_at	5.27174e-005
minnow_at	0.00064679
TA100_10RLI	negative
TA100_NA	negative
TA1535_10RLI	negative
TA1535_NA	negative

TA1535_10RLI	negative
TA1535_NA	negative
R6.-	
algae_at	0.00177907
Ames_test non-mutagen	
Carcino_Mouse	negative
Carcino_Rat	negative
daphnia_at	0.00291618
hERG_inhibition	medium_risk
medaka_at	3.47458e-005
minnow_at	0.000218316
TA100_10RLI	negative
TA100_NA	negative
TA1535_10RLI	negative
TA1535_NA	negative
R8.-	
algae_at	0.000893363
Ames_test mutagen	
Carcino_Mouse	negative
Carcino_Rat	negative
daphnia_at	0.000640968
hERG_inhibition	low_risk
medaka_at	2.05519e-006
minnow_at	1.17765e-005
TA100_10RLI	negative
TA100_NA	negative
TA1535_10RLI	negative
TA1535_NA	negative
R10.-	
algae_at	0.00102213
Ames_test mutagen	
Carcino_Mouse	positive
Carcino_Rat	negative
daphnia_at	0.000573745
hERG_inhibition	low_risk
medaka_at	1.40734e-006
minnow_at	1.5751e-005
TA100_10RLI	positive
TA100_NA	negative
TA1535_10RLI	negative
TA1535_NA	negative

Table S13. ADME - PreADMET | Prediction of ADME/Tox of compounds R1–R10.

R1.-	
BBB	0.123129
Buffer_solubility_mg_L	0.64161**
Caco2	36.1231
CYP_2C19_inhibition	Non
CYP_2C9_inhibition	Inhibitor
CYP_2D6_inhibition	Non
CYP_2D6_substrate	Non
CYP_3A4_inhibition	Non
CYP_3A4_substrate	Weakly
HIA	96.360606
MDCK	0.944234
Pgp_inhibition	Inhibitor
Plasma_Protein_Binding	90.172855
Pure_water_solubility_mg_L	0.0334635
Skin_Permeability	-2.48591
SKlogD_value	4.86141
SKlogP_value	4.86141
SKlogS_buffer	-5.935160**
SKlogS_pure	-7.21786
R3.-	
BBB	0.0496332
Buffer_solubility_mg_L	5.1182**
Caco2	39.8448

R2.-	
BBB	4.91546*
Buffer_solubility_mg_L	0.0591606**
Caco2	22.3311
CYP_2C19_inhibition	Non
CYP_2C9_inhibition	Inhibitor
CYP_2D6_inhibition	Non
CYP_2D6_substrate	Non
CYP_3A4_inhibition	Inhibitor
CYP_3A4_substrate	Substrate
HIA	96.986671
MDCK	0.0570201*
Pgp_inhibition	Inhibitor
Plasma_Protein_Binding	93.278806
Pure_water_solubility_mg_L	2.43839e-008
Skin_Permeability	-1.60589*
SKlogD_value	9.4002
SKlogP_value	9.4002
SKlogS_buffer	-6.991910**
SKlogS_pure	-13.37684
R4.-	
BBB	1.38253
Buffer_solubility_mg_L	19.3762**
Caco2	46.0642

CYP_2C19_inhibition	Non	CYP_2C19_inhibition	Non
CYP_2C9_inhibition	Inhibitor	CYP_2C9_inhibition	Inhibitor
CYP_2D6_inhibition	Non	CYP_2D6_inhibition	Non
CYP_2D6_substrate	Non	CYP_2D6_substrate	Non
CYP_3A4_inhibition	Inhibitor	CYP_3A4_inhibition	Non
CYP_3A4_substrate	Substrate	CYP_3A4_substrate	Weakly
HIA	93.180102	HIA	96.237543
MDCK	0.0448485	MDCK	13.1423
Pgp_inhibition	Inhibitor	Pgp_inhibition	Inhibitor
Plasma_Protein_Binding	86.248802	Plasma_Protein_Binding	100
Pure_water_solubility_mg_L	0.279233	Pure_water_solubility_mg_L	0.00294842
Skin_Permeability	-2.49455	Skin_Permeability	-1.94971
SKlogD_value	4.01101	SKlogD_value	6.1065
SKlogP_value	4.01101	SKlogP_value	6.1065
SKlogS_buffer	-5.019720**	SKlogS_buffer	-4.394480**
SKlogS_pure	-6.28287	SKlogS_pure	-8.21216
R5.-		R6.-	
BBB	0.0895296	BBB	0.0278881
Buffer_solubility_mg_L	0.917972**	Buffer_solubility_mg_L	1.09644**
Caco2	53.9079	Caco2	23.1843
CYP_2C19_inhibition	Non	CYP_2C19_inhibition	Non
CYP_2C9_inhibition	Inhibitor	CYP_2C9_inhibition	Inhibitor
CYP_2D6_inhibition	Non	CYP_2D6_inhibition	Non
CYP_2D6_substrate	Non	CYP_2D6_substrate	Non
CYP_3A4_inhibition	Non	CYP_3A4_inhibition	Non
CYP_3A4_substrate	Weakly	CYP_3A4_substrate	Substrate
HIA	97.737796	HIA	97.09432
MDCK	0.722555	MDCK	0.052716
Pgp_inhibition	Inhibitor	Pgp_inhibition	Inhibitor
Plasma_Protein_Binding	100	Plasma_Protein_Binding	90.67987
Pure_water_solubility_mg_L	0.00109602	Pure_water_solubility_mg_L	0.00727635
Skin_Permeability	-1.91053	Skin_Permeability	-3.31188
SKlogD_value	7.21402	SKlogD_value	5.84821
SKlogP_value	7.21402	SKlogP_value	5.84821
SKlogS_buffer	-5.715320**	SKlogS_buffer	-5.721730**
SKlogS_pure	-8.63833	SKlogS_pure	-7.8998
R7.-		R8.-	
BBB	1.97548	BBB	0.0183345
Buffer_solubility_mg_L	0.00748305	Buffer_solubility_mg_L	6.62834**
Caco2	50.7718	Caco2	49.1277
CYP_2C19_inhibition	Non	CYP_2C19_inhibition	Non
CYP_2C9_inhibition	Inhibitor	CYP_2C9_inhibition	Inhibitor
CYP_2D6_inhibition	Non	CYP_2D6_inhibition	Non
CYP_2D6_substrate	Non	CYP_2D6_substrate	Non
CYP_3A4_inhibition	Inhibitor	CYP_3A4_inhibition	Inhibitor
CYP_3A4_substrate	Substrate	CYP_3A4_substrate	Weakly
HIA	98.209709	HIA	96.743685
MDCK	7.43586*	MDCK	0.0691866*
Pgp_inhibition	Inhibitor	Pgp_inhibition	Inhibitor
Plasma_Protein_Binding	90.845069	Plasma_Protein_Binding	100
Pure_water_solubility_mg_L	0.000131292	Pure_water_solubility_mg_L	0.00183749
Skin_Permeability	-2.06696	Skin_Permeability	-2.41114*
SKlogD_value	6.45931	SKlogD_value	6.83341
SKlogP_value	6.45931	SKlogP_value	6.83341
SKlogS_buffer	-7.8754	SKlogS_buffer	-4.947030**
SKlogS_pure	-9.63124	SKlogS_pure	-8.50421
R9.-		**R10**.-	
BBB	0.318423	BBB	2.66944
Buffer_solubility_mg_L	10.3431**	Buffer_solubility_mg_L	5.79925
Caco2	18.4773	Caco2	23.3819
CYP_2C19_inhibition	Non	CYP_2C19_inhibition	Non
CYP_2C9_inhibition	Inhibitor	CYP_2C9_inhibition	Inhibitor
CYP_2D6_inhibition	Non	CYP_2D6_inhibition	Non
CYP_2D6_substrate	Non	CYP_2D6_substrate	Non
CYP_3A4_inhibition	Inhibitor	CYP_3A4_inhibition	Inhibitor
CYP_3A4_substrate	Substrate	CYP_3A4_substrate	Substrate
HIA	91.805294	HIA	98.6335
MDCK	4.39826	MDCK	0.0581581*
Pgp_inhibition	Inhibitor	Pgp_inhibition	Inhibitor

Plasma_Protein_Binding	91.723294
Pure_water_solubility_mg_L	0.0309251
Skin_Permeability	-2.80001*
SKlogD_value	4.76377
SKlogP_value	4.76377
SKlogS_buffer	-4.732440**
SKlogS_pure	-7.25678

Plasma_Protein_Binding	96.977388
Pure_water_solubility_mg_L	0.00016586
Skin_Permeability	-1.75733*
SKlogD_value	6.83969
SKlogP_value	6.83969
SKlogS_buffer	-4.98917
SKlogS_pure	-9.5328

Table S14. Properties predicted by PhysChem - ACD/Labs of compounds R1–R10.

R1.-	
Density:	1.3±0.1 g/cm3
Boiling Point:	823.7±65.0 °C at 760 mmHg
Vapour Pressure:	0.0±3.0 mmHg at 25°C
Enthalpy of Vaporization:	119.7±3.0 kJ/mol
Flash Point:	451.9±34.3 °C
Index of Refraction:	1.653
Molar Refractivity:	158.0±0.3 cm3
#H bond acceptors:	8
#H bond donors:	2
#Freely Rotating Bonds:	10
#Rule of 5 Violations:	1
ACD/LogP:	4.43
ACD/LogD (pH 5.5):	4.49
ACD/BCF (pH 5.5):	1512.25
ACD/KOC (pH 5.5):	6570.06
ACD/LogD (pH 7.4):	4.49
ACD/BCF (pH 7.4):	1512.3
ACD/KOC (pH 7.4):	6570.27
Polar Surface Area:	95 Å2
Polarizability:	62.6±0.5 10-24cm3
Surface Tension:	53.0±3.0 dyne/cm
Molar Volume:	431.9±3.0 cm3

R2.-	
Density :	1.2±0.1 g/cm3
Boiling Point:	675.2±55.0 °C at 760 mmHg
Vapour Pressure :	0.0±2.1 mmHg at 25°C
Enthalpy of Vaporization:	99.1±3.0 kJ/mol
Flash Point:	362.1±31.5 °C
Index of Refraction:	1.637
Molar Refractivity:	175.0±0.5 cm3
#H bond acceptors:	8
#H bond donors:	2
#Freely Rotating Bonds:	8
#Rule of 5 Violations:	2
ACD/LogP:	8.18
ACD/LogD (pH 5.5):	7.78
ACD/BCF (pH 5.5):	479472.53
ACD/KOC (pH 5.5):	405380.16
ACD/LogD (pH 7.4):	7.78
ACD/BCF (pH 7.4):	479464.09
ACD/KOC (pH 7.4):	405373.03
Polar Surface Area:	108 Å2
Polarizability:	69.4±0.5 10-24cm3
Surface Tension:	46.0±7.0 dyne/cm
Molar Volume:	487.8±7.0 cm3

R3.-	
Density:	1.2±0.1 g/cm3
Boiling Point:	762.4±60.0 °C at 760 mmHg
Vapour Pressure:	0.0±2.6 mmHg at 25°C
Enthalpy of Vaporization:	111.0±3.0 kJ/mol
Flash Point:	414.9±32.9 °C
Index of Refraction:	1.605
Molar Refractivity:	148.1±0.3 cm3
#H bond acceptors:	10
#H bond donors:	3
#Freely Rotating Bonds:	12
#Rule of 5 Violations:	2
ACD/LogP:	4.01
ACD/LogD (pH 5.5):	3.27
ACD/BCF (pH 5.5):	180.94
ACD/KOC (pH 5.5):	1437.3
ACD/LogD (pH 7.4):	3.27
ACD/BCF (pH 7.4):	180.94
ACD/KOC (pH 7.4):	1437.29
Polar Surface Area:	124 Å2
Polarizability:	58.7±0.5 10-24cm3
Surface Tension:	49.2±3.0 dyne/cm
Molar Volume:	430.3±3.0 cm3

R4.-	
Density:	1.2±0.1 g/cm3
Boiling Point:	765.6±60.0 °C at 760 mmHg
Vapour Pressure:	0.0±2.6 mmHg at 25°C
Enthalpy of Vaporization:	111.5±3.0 kJ/mol
Flash Point:	416.8±32.9 °C
Index of Refraction:	1.645
Molar Refractivity:	141.5±0.3 cm3
#H bond acceptors:	6
#H bond donors:	2
#Freely Rotating Bonds:	9
#Rule of 5 Violations:	1
ACD/LogP:	6.53
ACD/LogD (pH 5.5):	5.89
ACD/BCF (pH 5.5):	17581.53
ACD/KOC (pH 5.5):	38036.09
ACD/LogD (pH 7.4):	5.89
ACD/BCF (pH 7.4):	17581.88
ACD/KOC (pH 7.4):	38036.84
Polar Surface Area:	77 Å2
Polarizability:	56.1±0.5 10-24cm3
Surface Tension:	51.9±3.0 dyne/cm
Molar Volume:	390.2±3.0 cm3

R5.-	
Density:	1.2±0.1 g/cm3
Boiling Point:	
Vapour Pressure:	
Enthalpy of Vaporization:	
Flash Point:	
Index of Refraction:	1.662
Molar Refractivity:	145.1±0.5 cm3
#H bond acceptors:	5
#H bond donors:	1
#Freely Rotating Bonds:	7
#Rule of 5 Violations:	1

R6.-	
Density:	1.4±0.1 g/cm3
Boiling Point:	
Vapour Pressure:	
Enthalpy of Vaporization:	
Flash Point:	
Index of Refraction:	1.682
Molar Refractivity:	159.4±0.5 cm3
#H bond acceptors:	9
#H bond donors:	2
#Freely Rotating Bonds:	11
#Rule of 5 Violations:	2

ACD/LogP:	7.82
ACD/LogD (pH 5.5):	6.36
ACD/BCF (pH 5.5):	40195.15
ACD/KOC (pH 5.5):	68744.55
ACD/LogD (pH 7.4):	6.36
ACD/BCF (pH 7.4):	40199.12
ACD/KOC (pH 7.4):	68751.35
Polar Surface Area:	85 Å2
Polarizability:	57.5±0.5 10-24cm3
Surface Tension:	49.7±7.0 dyne/cm
Molar Volume:	392.2±7.0 cm3

ACD/LogP:	6.91
ACD/LogD (pH 5.5):	5.05
ACD/BCF (pH 5.5):	4037.03
ACD/KOC (pH 5.5):	13268.15
ACD/LogD (pH 7.4):	5.05
ACD/BCF (pH 7.4):	4037.06
ACD/KOC (pH 7.4):	13268.24
Polar Surface Area:	161 Å2
Polarizability:	63.2±0.5 10-24cm3
Surface Tension:	55.3±7.0 dyne/cm
Molar Volume:	420.5±7.0 cm3

R7.-

Density:	1.4±0.1 g/cm3
Boiling Point:	722.2±70.0 °C at 760 mmHg
Vapour Pressure:	0.0±2.3 mmHg at 25°C
Enthalpy of Vaporization:	105.5±3.0 kJ/mol
Flash Point:	390.6±35.7 °C
Index of Refraction:	1.673
Molar Refractivity:	155.6±0.4 cm3
#H bond acceptors:	7
#H bond donors:	0
#Freely Rotating Bonds:	12
#Rule of 5 Violations:	2
ACD/LogP:	5.27
ACD/LogD (pH 5.5):	4.64
ACD/BCF (pH 5.5):	1997.15
ACD/KOC (pH 5.5):	8017.33
ACD/LogD (pH 7.4):	4.64
ACD/BCF (pH 7.4):	1997.15
ACD/KOC (pH 7.4):	8017.33
Polar Surface Area:	132 Å2
Polarizability:	61.7±0.5 10-24cm3
Surface Tension:	67.2±5.0 dyne/cm
Molar Volume:	414.8±5.0 cm3

R8.-

Density:	1.3±0.1 g/cm3
Boiling Point:	804.8±65.0 °C at 760 mmHg
Vapour Pressure:	0.0±2.9 mmHg at 25°C
Enthalpy of Vaporization:	117.0±3.0 kJ/mol
Flash Point:	440.6±34.3 °C
Index of Refraction:	1.706
Molar Refractivity:	170.5±0.3 cm3
#H bond acceptors:	6
#H bond donors:	2
#Freely Rotating Bonds:	9
#Rule of 5 Violations:	2
ACD/LogP:	6.87
ACD/LogD (pH 5.5):	6.29
ACD/BCF (pH 5.5):	35293.42
ACD/KOC (pH 5.5):	62634.34
ACD/LogD (pH 7.4):	6.29
ACD/BCF (pH 7.4):	35296.25
ACD/KOC (pH 7.4):	62639.36
Polar Surface Area:	140 Å2
Polarizability:	67.6±0.5 10-24cm3
Surface Tension:	62.8±3.0 dyne/cm
Molar Volume:	438.3±3.0 cm3

R9.-

Density:	1.3±0.1 g/cm3
Boiling Point:	820.9±65.0 °C at 760 mmHg
Vapour Pressure:	0.0±3.1 mmHg at 25°C
Enthalpy of Vaporization:	123.4±3.0 kJ/mol
Flash Point:	450.2±34.3 °C
Index of Refraction:	1.66
Molar Refractivity:	153.7±0.3 cm3
#H bond acceptors:	10
#H bond donors:	4
#Freely Rotating Bonds:	12
#Rule of 5 Violations:	2
ACD/LogP:	4.15
ACD/LogD (pH 5.5):	3.61
ACD/BCF (pH 5.5):	327.32
ACD/KOC (pH 5.5):	2196.58
ACD/LogD (pH 7.4):	3.6
ACD/BCF (pH 7.4):	317.64
ACD/KOC (pH 7.4):	2131.6
Polar Surface Area:	136 Å2
Polarizability:	60.9±0.5 10-24cm3
Surface Tension:	58.7±3.0 dyne/cm
Molar Volume:	416.7±3.0 cm3

R10.-

Density:	1.3±0.1 g/cm3
Boiling Point:	742.6±70.0 °C at 760 mmHg
Vapour Pressure:	0.0±2.5 mmHg at 25°C
Enthalpy of Vaporization:	108.3±3.0 kJ/mol
Flash Point:	402.9±35.7 °C
Index of Refraction:	1.637
Molar Refractivity:	161.2±0.5 cm3
#H bond acceptors:	8
#H bond donors:	0
#Freely Rotating Bonds:	10
#Rule of 5 Violations:	2
ACD/LogP:	6.18
ACD/LogD (pH 5.5):	5.55
ACD/BCF (pH 5.5):	9740.59
ACD/KOC (pH 5.5):	24923.9
ACD/LogD (pH 7.4):	5.55
ACD/BCF (pH 7.4):	9740.82
ACD/KOC (pH 7.4):	24924.5
Polar Surface Area:	122 Å2
Polarizability:	63.9±0.5 10-24cm3
Surface Tension:	51.2±7.0 dyne/cm
Molar Volume:	449.0±7.0 cm3